

# UNCLASSIFIED

AD NUMBER	
ADC000419	
CLASSIFICATION CHANGES	
TO:	unclassified
FROM:	confidential
LIMITATION CHANGES	
TO:	Approved for public release, distribution unlimited
FROM:	Distribution authorized to U.S. Gov't. agencies and their contractors; Administrative/Operational Use; AUG 1974. Other requests shall be referred to Office of Naval Research, Attn: Code 102-OSC, Arlington, VA 22217.
AUTHORITY	
31 Aug 1986, DoDD 5200.10; CNO/N772 ltr N772A/6U875630 20 Jan 2006 and ONR ltr 31 Jan 2006	

THIS PAGE IS UNCLASSIFIED

**CONFIDENTIAL**

NOO TR-244

# IOMEDEX Sound Velocity Analysis and Environmental Data Summary

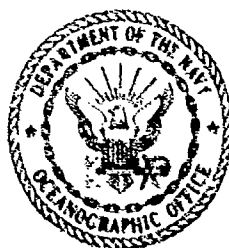
[Unclassified Title]

DON F. FENNER, KENNETH W. LACKIE,  
BENJAMIN A. WATROUS AND LOUIS A. BANCHERO

*Naval Oceanographic Office*

August 1974

Provisional Technical Report



"NATIONAL SECURITY INFORMATION"  
"Unauthorized Disclosure Subject to Criminal  
Sanctions"

Prepared for the  
Long Range Acoustic Propagation Project  
Office of Naval Research Code 102-OSR  
Arlington, Va. 22217

DEPARTMENT OF THE NAVY  
NAVAL OCEANOGRAPHIC OFFICE  
Washington, D.C. 20373

DDC  
RECEIVED  
JUL 20 1974  
RECEIVED

**CONFIDENTIAL**

CONFIDENTIAL, classified by CNR  
Subject to GDS of E.O. 11652  
Auto downgraded at 2 yr intervals and  
declassified Dec. 31, 1988

**CONFIDENTIAL**

**NATIONAL SECURITY INFORMATION**

Unauthorized Disclosure Subject to Criminal Sanctions.

*Littleton file*

*9*

**CONFIDENTIAL**

**CONFIDENTIAL**

UNCLASSIFIED


SECURITY CLASSIFICATION OF THIS PAGE (When Data Entered)

REPORT DOCUMENTATION PAGE		READ INSTRUCTIONS BEFORE COMPLETING FORM
1. REPORT NUMBER N00TR-244	2. GOVT ACCESSION NO.	3. RECIPIENT'S CATALOG NUMBER
4. TITLE (and Subtitle) IOMEDEX SOUND VELOCITY ANALYSIS AND ENVIRONMENTAL DATA SUMMARY (U)		5. TYPE OF REPORT & PERIOD COVERED Provisional
6. AUTHOR(s) Don F. Jenner, Kenneth W. Lackie, Benjamin A. Watrous and Louis A. Banchemo		6. PERFORMING ORG. REPORT NUMBER
9. PERFORMING ORGANIZATION NAME AND ADDRESS Naval Oceanographic Office Code 6150 Washington, DC 20373		8. CONTRACT OR GRANT NUMBER(s)
10. CONTROLLING OFFICE NAME AND ADDRESS Long Range Acoustic Propagation Project Office of Naval Research Code 102-OSC Arlington, Virginia 22217		10. PROGRAM ELEMENT, PROJECT, TASK AREA & WORK UNIT NUMBERS 714-LW-RGA
11. MONITORING AGENCY NAME & ADDRESS (if different from Controlling Office)		12. REPORT DATE August 1974
		13. NUMBER OF PAGES 62
		14. SECURITY CLASS. (of this report) CONFIDENTIAL
		15. DECLASSIFICATION/DOWNGRADING SCHEDULE GDS 1980
16. DISTRIBUTION STATEMENT (of this Report) In addition to security requirements which apply to this document and must be met, it may be further distributed to the holder only with the prior approval of the Director, Long Range Acoustic Propagation Project		
17. DISTRIBUTION STATEMENT (of the abstract entered in Block 20, if different from Report)		
18. SUPPLEMENTARY NOTES		
19. KEY WORDS (Continue on reverse side if necessary and identify by block number) Oceanographic data, current meter data, weather data, bathymetric tracks, sound velocity profiles, deep sound channel axis, critical depth, mixed layer depth, Mediterranean Sea, Ionian Sea, Levantine Intermediate Water, Maltese Front, LRAPP (Long Range Acoustic Propagation Project)		
20. ABSTRACT (Continue on reverse side if necessary and identify by block number) During the Ionian Mediterranean Exercise (IOMEDEX) in November 1971, a total of 581 oceanographic observations were collected in the Ionian Basin of the Mediterranean Sea along with continuous bathymetric and weather observations. Two taut-line current measuring arrays were implanted in the northern and central Ionian Sea. Most oceanographic data were collected with expendable bathythermographs (XBTs) and converted into sound velocity profiles. Sea surface temperatures and mixed layer depth patterns are defined before and		

UNCLASSIFIED

SECURITY CLASSIFICATION OF THIS PAGE (When Data Entered)

after a large storm on 19-23 November. Basic temporal changes in sound velocity structure are defined at three points in the Ionian Sea, and spatial changes in sound velocity are defined along several specific tracks. The deep sound channel (DSC) axis varied between 90 and 300 m (average of about 150 m) with sound velocities between about 1512 and 1518 m/sec. High-salinity Levantine Intermediate Water was the primary oceanographic influence on DSC structure and on secondary sound channels found below DSC axis. Critical depth decreased during IOMEDEX as a result of autumnal cooling. The Maltese Front was detected in the central Ionian Sea, but could not be defined accurately owing to the lack of synoptic sea surface temperature data.



UNCLASSIFIED

UNCLASSIFIED

#### ACKNOWLEDGMENTS

The authors wish to acknowledge the analytical aid of Paul J. Bucca, Undersea Surveillance Oceanographic Center, NAVOCEANO in preparing the figures on sea surface temperature and mixed layer depth, and that of Reuben J. Busch for providing the bathymetric cross sections used in this report.

The illustrations were prepared by Joanne V. Lackie, Visual Information Support Group. Bernadine Heit and Judy Albritten are thanked for typing this manuscript.

UNCLASSIFIED

## CONTENTS

	Page
ABSTRACT. . . . .	i
ACKNOWLEDGMENTS . . . . .	iii
FIGURES . . . . .	vii
TABLES. . . . .	vii
APPENDIXES. . . . .	vii
INTRODUCTION. . . . .	1
DISCUSSION OF ENVIRONMENTAL DATA	
A. Data Availability and Measurement System Performance. . .	1
B. Treatment of Data . . . . .	9
C. Distribution of Oceanographic Data. . . . .	9
GENERAL OCEANOGRAPHY AS RELATED TO SOUND VELOCITY STRUCTURE . . .	10
NEAR-SURFACE THERMAL STRUCTURE	
A. Sea Surface Temperature . . . . .	13
B. Mixed Layer Depth . . . . .	17
SOUND VELOCITY STRUCTURE	
A. Temporal Variability at Points A, B, and C. . . . .	17
B. Sound Velocity Structure Between Points A and C . . . . .	24
C. Sound Velocity Structure Between Points A and B . . . . .	27
CURRENT MEASUREMENTS. . . . .	30
SEA, SWELL, AND WEATHER OBSERVATIONS. . . . .	34
SUMMARY . . . . .	36
REFERENCES. . . . .	39
DISTRIBUTION LIST . . . . .	53

Best Available Copy

PRECEDING PAGE BLANK-NOT FILMED

## FIGURES

	Page
1. Location of IOMEDEX Reference Points and Historical Salinity Measurements. . . . .	2
2. Location of SVPs and XBTs Deeper Than 760 Meters . . . . .	5
3. Location of XBTs Between 460 Meters and 760 Meters . . . . .	6
4. Location of XBTs Shallower Than 460 Meters . . . . .	7
5. Location of AXBTs. . . . .	8
6. Historical Autumn Temperature-Salinity-Sound Velocity-Density Profiles and T-S Comparison for Central Ionian Basin . . . .	11
7. Positions of Oceanic Fronts in Ionian Sea. . . . .	12
8. Average Monthly Critical Depths for Central and Southern Ionian Basin . . . . .	14
9. Sea Surface Temperature ( $^{\circ}\text{C}$ ) for 8-14 November . . . . .	15
10. Sea Surface Temperature ( $^{\circ}\text{C}$ ) for 23-26 November. . . . .	16
11. Mixed Layer Depth (m) for 11-14 November . . . . .	18
12. Mixed Layer Depth (m) for 23-26 November . . . . .	19
13. Time-series Plot of Sound Velocity at Point A (31 Oct-26 Nov). . . . .	20
14. Time-series Plot of Sound Velocity at Point B (1-21 Nov) . . . . .	22
15. Time-series Plot of Sound Velocity at Point C (7-25 Nov) . . . . .	23
16. Sound Velocity Profiles from Point A to Point C (7-15 Nov) . . . . .	25
17. Sound Velocity Cross Section from Point A to Point C (7-15 Nov) . . . . .	26
18. Sound Velocity Profiles from Point B to Point A (10-20 Nov). . . . .	28
19. Sound Velocity Cross Section from Point B to Point A (10-20 Nov). . . . .	29



UNCLASSIFIED

FIGURES (CONTINUED)

	Page
20. Current Meter Array 1, Point A - 36°16'N, 17°19'E. . . . .	31
21. Current Meter Array 2, Point C - 38°39'N, 18°16'E. . . . .	32
22. Wind Force, Wind Direction, Sea State, and Swell Height Summary . . . . .	35

TABLES

1. SANDS SVP Observations . . . . .	4
2. Summary of IOMEDEX Current Meter Data. . . . .	33

APPENDIXES

A. Glossary . . . . .	43
B. Hourly Averages of Current Meter Measurements. . . . .	45

## CONFIDENTIAL

### INTRODUCTION

(C) The Ionian Mediterranean Exercise (IOMEDEX) was conducted in the Ionian Sea and in immediately adjacent regions of the Mediterranean Sea during October-November 1971. The following ships participated in the exercise:

- USNS SANDS (T-AGOR-6)
- R/V KNORR
- R/V NORTH SEAL
- USS HAMMERBERG (DE 1015)
- USS COURTNEY (DE 1021)
- USS LESTER (DE 1022)

Oceanographic data were collected from all six ships and from various aircraft for use in determining environmental effects on acoustic propagation in the Ionian Basin. Continuous bathymetric records were made by SANDS, KNORR, and NORTH SEAL between points A and B, A and C, and B and C (see figure 1) and by HAMMERBERG, COURTNEY, and LESTER throughout the northern and central Ionian Basin. In addition, NAVOCEANO implanted and recovered two taut-line, self-contained current meter arrays near points A and C. Details on the exact nature of the exercise can be found in the IOMEDEX LRAPP Operation Order (Maury Center for Ocean Science, 1971). Much of the analysis contained in this report has appeared previously in the IOMEDEX Synopsis Report (Maury Center for Ocean Science, 1972a) and in the IOMEDEX Summary Report (Maury Center for Ocean Science, 1973). Various acronyms and oceanographic terms used in this report are defined in appendix A.

### DISCUSSION OF ENVIRONMENTAL DATA

#### A. Data Availability and Measurement System Performance

(U) The following types of oceanographic data were collected during IOMEDEX:

- Expendable bathythermographs (XBTs)
- Airborne expendable bathythermographs (AXBTs)
- Sound velocimeter profiles (SVPs)
- Current speed and direction
- Sea state and swell height
- Wind speed and direction

UNCLASSIFIED

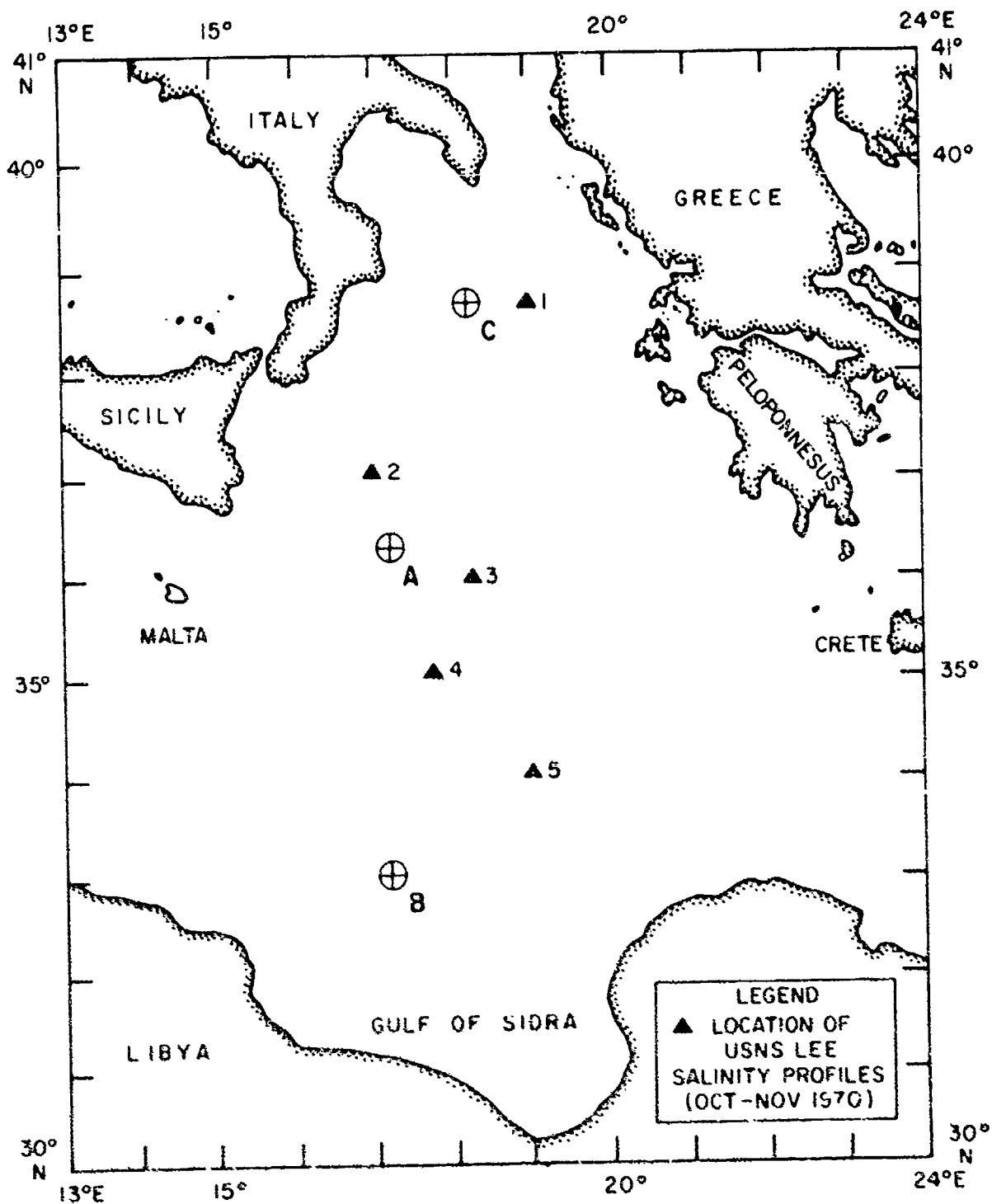


Figure 1. Location of IONDEX Reference Points and Historical Salinity Measurements

UNCLASSIFIED

UNCLASSIFIED

XBT data were collected using Sippican Model T-4 probes (460 m), T-5 probes (1830 m), and T-7 probes (760 m). AXBT data were collected to a maximum depth of 330 m using AN/SSQ-36 probes. Current and meteorological data collection were discussed in detail in separate sections below.

(U) Between 26 October and 27 November, 82 T-5 and 231 T-7 XBT traces were collected by SANDS, KNORR, and NORTH SEAL. During this same period, HAMMERBERG, COURTNEY, and LESTER collected 91 T-4 XBT traces. Between 12 and 23 November, P-3 aircraft from Patrol Squadron 16, operating from the U.S. Naval Facility at Sigonella, Sicily, collected 153 AXBT traces on 14 flights. In addition, SANDS occupied 19 sound velocimeter stations during IOMEDX. Each station produced two SVPs, one for the lowering and one for the retrieval. Locations and maximum depths of these SVPs are given in table 1.

(U) Figure 2 shows the locations of the 19 SVP stations occupied by SANDS and the location of T-5 XBTs that extended to depths greater than 760 m. These observations are concentrated along a line running through points A, B, and C. Figure 3 shows locations of XBTs with maximum depths between 460 and 760 m. Most of these observations were collected using T-7 probes in the western Ionian Basin; locations of T-5 probes that failed at depths less than 760 m are also included in this figure. Figure 4 shows locations of XBT observations extending to less than 460 m. Most of these observations were collected with T-4 probes in the northern and central Ionian Basin; figure 4 also shows T-5 and T-7 observations shallower than 460 m depth. Figure 5 shows locations of AXBT observations collected throughout the Ionian Sea during IOMEDX. The majority of observations shown in figures 2 through 5 extend deeper than the maximum autumn depth of the deep sound channel (DSC) axis in the Ionian Sea (approximately 250 m, Fenner, 1968).

(U) Many T-5 XBTs dropped during IOMEDX did not function reliably. Although no records were kept of the exact number that completely malfunctioned, it is estimated that about two-thirds of the probes failed completely. Of the 82 T-5 traces judged to be "good" (usable trace to at least 100 m), only 34 (41%) were valid to their 1830-m maximum depth. Twenty-five T-5s considered "good" did not reach 760 m. Comparable data for the T-7 probes indicate much better performance. More than 80% of these probes were "good", and 196 (85%) of the 231 observations were valid to 760 m. No performance data are available for the T-4 XBTs.

(U) Of the 204 AXBTs dropped, 153 (75%) produced usable temperature traces, with most recordings to 330 m. However, the majority of the AXBT traces were offset towards higher temperatures by a variable increment. Therefore, AXBT data could not be used for sea surface temperature or sound velocity analyses. Nevertheless, AXBTs did give accurate values of mixed layer depth.

UNCLASSIFIED

UNCLASSIFIED

Station Number	Date (1971)	Time (Z)	Lat (N)	Long (E)	Maximum Depth (m)	Near Ref Point
0	31 Oct	0630	36°32'	17°30'	1889	A
B	1 Nov	1200	32°57'	17°38'	2982	B
1	7 Nov	1200	36°18'	17°16'	1857	A
2	7 Nov	1400	36°24'	17°17'	1847	A
3	8 Nov	2130	35°25'	17°30'	1796	
4	9 Nov	0800	35°30'	17°31'	1835	
5	10 Nov	0800	34°15'	17°33'	1886	
6	10 Nov	2130	32°56'	17°29'	1817	B
7	11 Nov	1330	33°02'	17°31'	1875	B
8	12 Nov	0700	34°11'	17°22'	2468	
9	12 Nov	1245	34°11'	17°22'	2307	
10	13 Nov	0309	35°25'	17°34'	3541	
11	13 Nov	1440	35°24'	17°34'	2849	
12	14 Nov	0800	36°23'	17°20'	3200	A
13	17 Nov	1700	36°21'	17°15'	3186	A
14	18 Nov	1800	35°58'	16°04'	3495	
15	19 Nov	1200	36°02'	17°29'	3495	
16	22 Nov	0348	38°40'	16°10'	2502	C
17	23 Nov	2000	36°25'	17°10'	3006	A

Table 1. SANDS SVP Observations

UNCLASSIFIED

UNCLASSIFIED

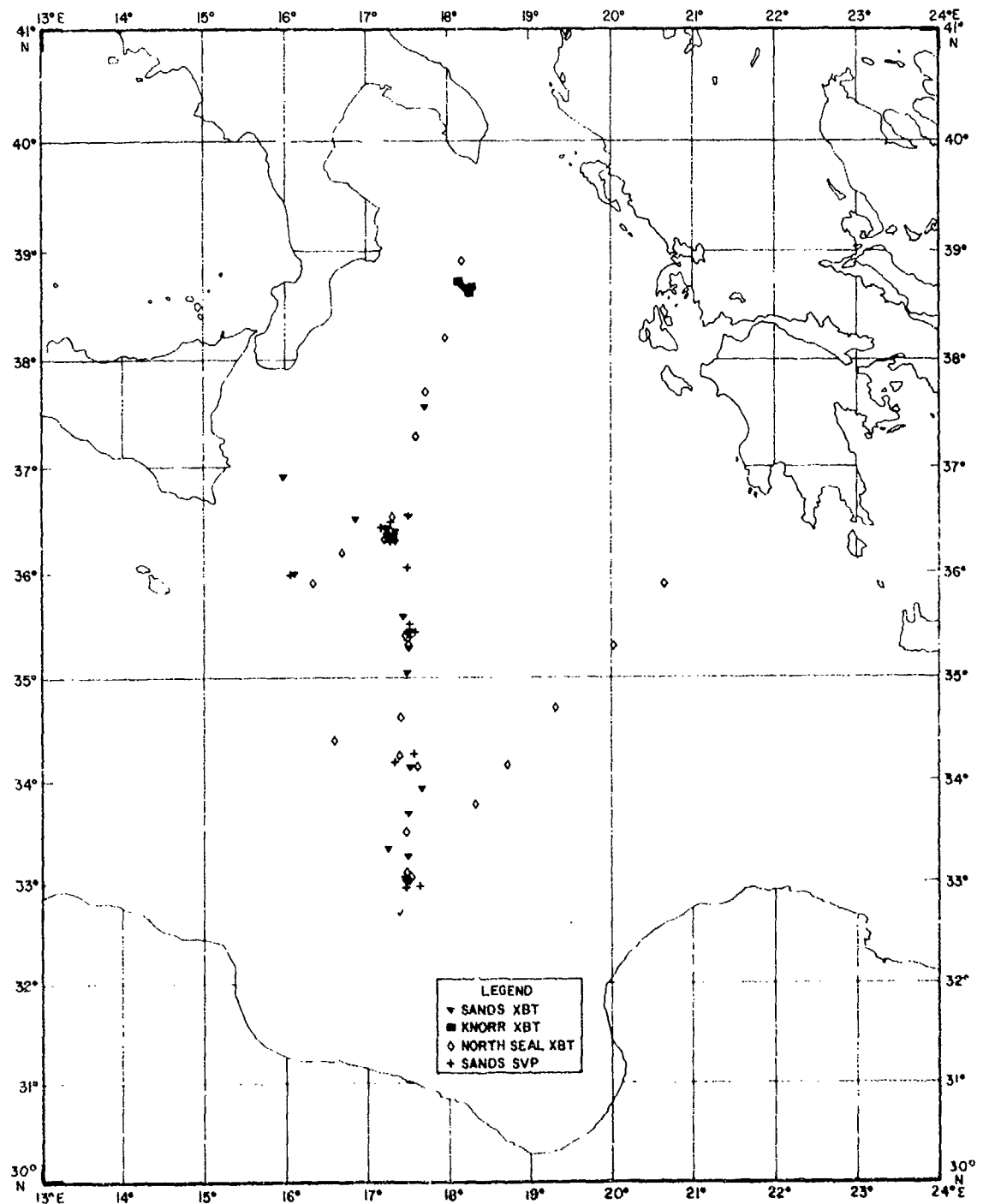


Figure 2. Location of SVPs and XBTs Deeper Than 760 Meters

UNCLASSIFIED

UNCLASSIFIED

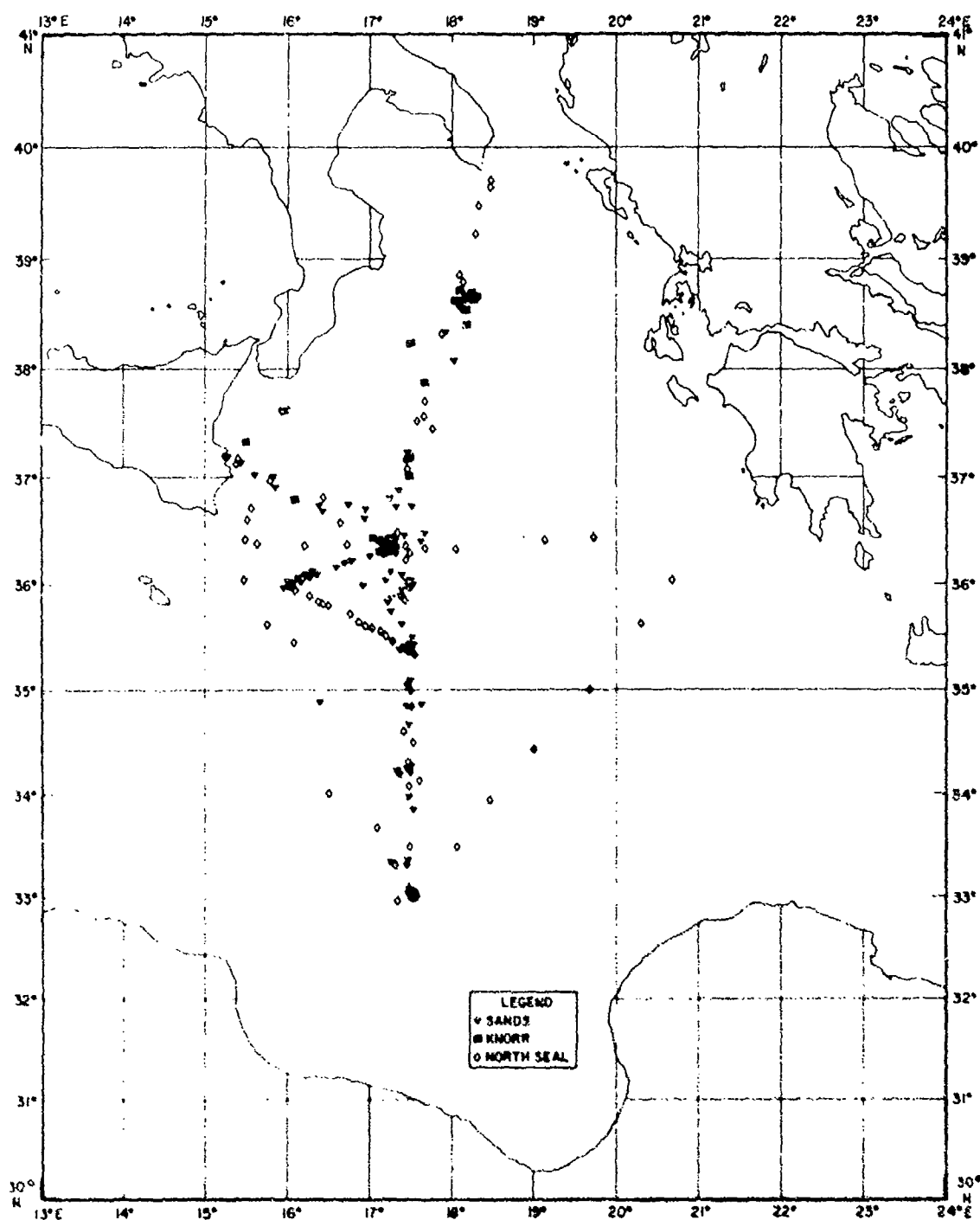


Figure 3. Location of XBTs Between 460 and 760 Meters

UNCLASSIFIED

UNCLASSIFIED

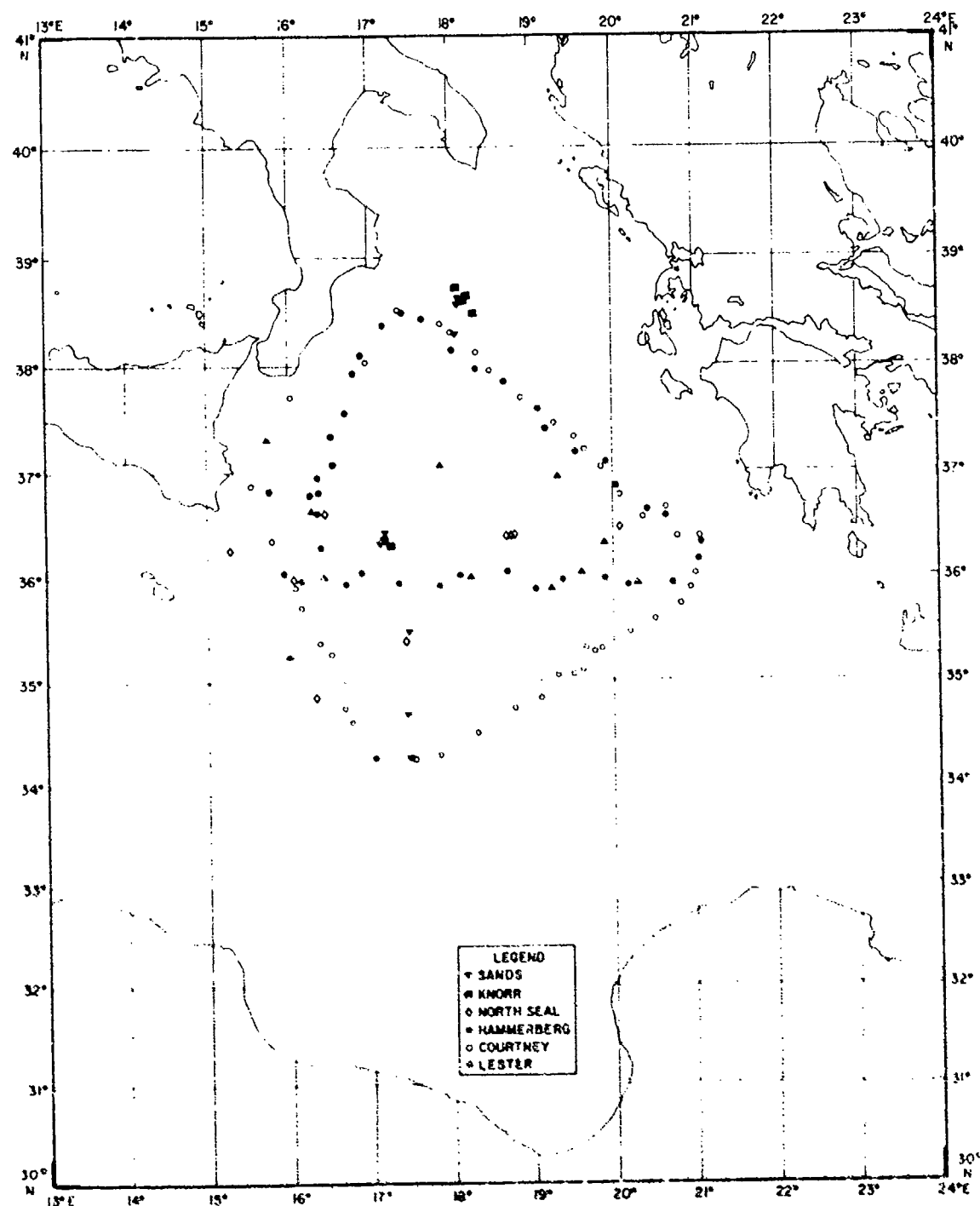


Figure 4. Location of XBIs Shallower Than 460 Meters

UNCLASSIFIED



UNCLASSIFIED

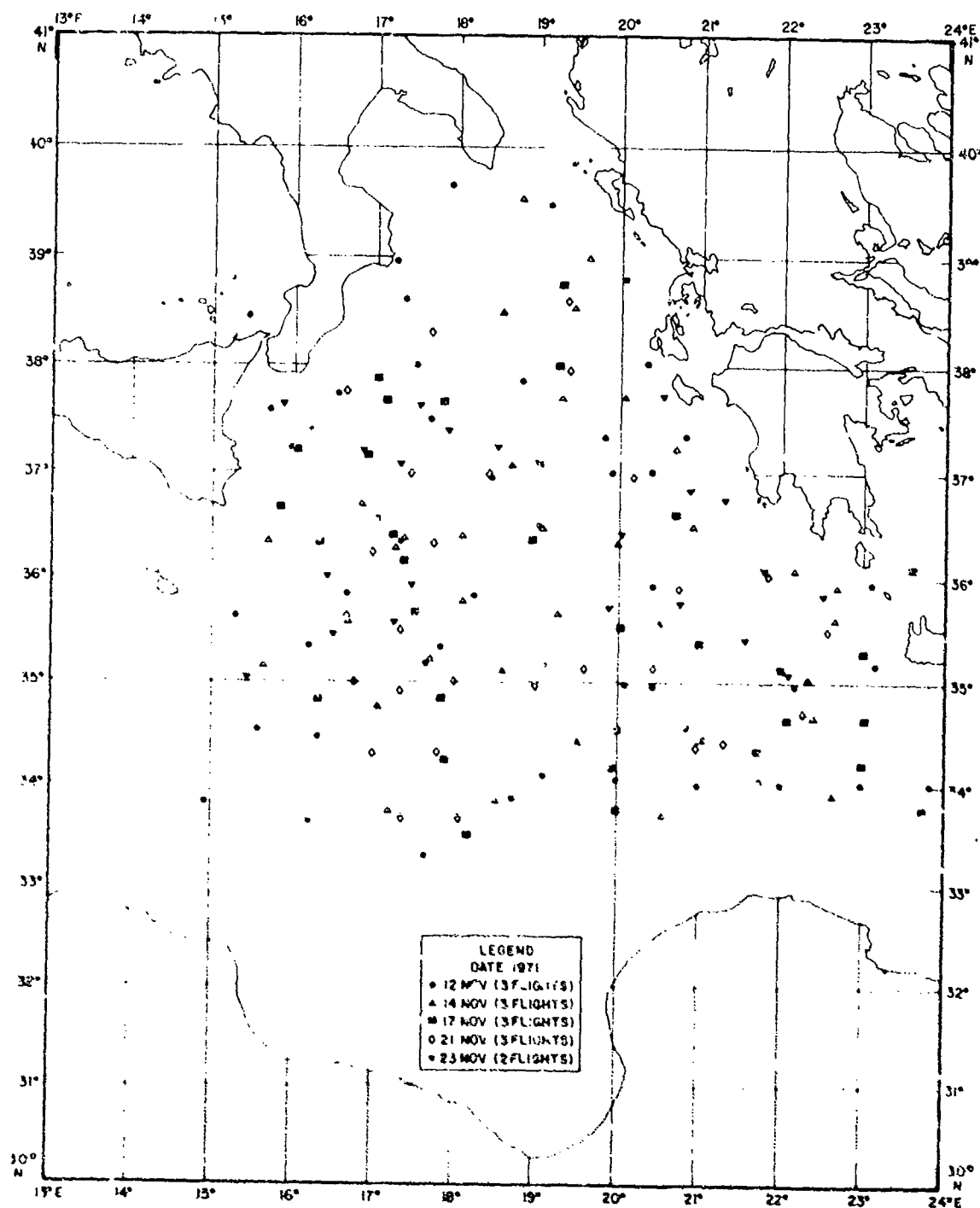


Figure 5. Location of AXBFe

UNCLASSIFIED

## UNCLASSIFIED

### B. Treatment of Data

(U) The majority of sound velocity data used in this report were calculated from XBT traces and historical salinity values using the equation of Wilson (1960). Selected XBT traces were hand digitized at temperature inflection points. Salinity correction factors selected for use in Wilson's equation were derived at salinity profile inflection points and at preset 100-m depth intervals from data collected by USNS LEE during October and November 1970 as part of IMP (figure 1 shows locations of LEE observations). Sound velocity profiles were calculated using either the nearest LEE salinity profile or an average of the nearest two adjacent LEE salinity profiles. Sound velocity profiles presented in this report were not extrapolated below the depth of actual measurement. All bottom depths have been corrected for variations from a standard sound velocity of 1500 m/sec using depth correction tables of Matthews (1939).

### C. Distribution of Oceanographic Data

(U) Although a large quantity of temperature and sound velocity data were collected during IOMEDEX, the major data collection effort supported acoustic measurements. Therefore, the vast majority of temperature and sound velocity data were taken synoptically with various scheduled acoustic runs. The nature of the exercise required all ships to follow predetermined schedules during acoustic operations, and little time could be devoted exclusively to collection of other oceanographic data. Thus, XBT and SVP data were collected at various reference points and along various tracks only when one of the ships was conducting acoustic operations. For example, oceanographic data were collected at point A only during 5-8 November, 12-15 November, and after 23 November, leaving large gaps in the overall data record at this location. These temporal data gaps are even more pronounced at points B and C. To further complicate matters, the IOMEDEX area was under the influence of a large storm during the period 19-23 November (see discussion of weather observations). This depression markedly changed near-surface characteristics through mixing and consequently divides IOMEDEX into two time periods, one before and one after the storm. The data base before the storm (1-19 November) is considerably larger and better distributed than after the storm (23-31 November).

(U) Oceanographic data densities generally were inadequate to resolve short-term temporal and spatial variations in sound velocity structure at points A, B, or C. Similarly, it was impossible to locate near-surface features such as oceanographic fronts with any degree of accuracy based on IOMEDEX data alone. Because of the small data base after the storm, near-surface thermal characteristics after the storm can be described only in a relatively small region between about 35° and 39°N. Because of the overall nature of the IOMEDEX data base, sound velocity analyses for this report have been restricted to temporal studies at points A, B, and C and to studies of spatial variability along the B-A and A-C tracks.

UNCLASSIFIED

#### GENERAL OCEANOGRAPHY AS RELATED TO SOUND VELOCITY STRUCTURE

(U) The Ionian Basin is fairly complex oceanographically and is characterized by a relatively changeable surface and near-surface layer (0 to 100 m), an intermediate layer denoted by a strong salinity maximum (100 to about 500 m), and an extremely stable deep layer that is nearly isothermal and isohaline. Figure 6 shows typical autumn temperature, salinity, density, and sound velocity profiles and a T-S curve for the central Ionian Basin.

(U) Levantine Intermediate Water (LIW) is the most important water mass affecting sound velocity in the Ionian Basin. This water mass is characterized by a strong salinity maximum (38.7 to 39.0 ‰ in the Ionian Basin) at depths between 200 and 600 m (Wust, 1961). The deep sound channel (DSC) axis generally occurs between the bottom of the seasonal thermocline and the depth of the LIW core. A preferential flow of LIW across the Ionian Basin occurs between 34° and 35°N according to Wust. Other strong flows of this water mass occur along about 33°N and east of about 17°E along the coast of Peloponnesus (Moskalenko and Ovchinnikov, 1965). Generally, unmixed concentrations of LIW are greater in regions of preferential LIW flow. However, substantial quantities of LIW are present in most of the Ionian Basin throughout the year as shown on the salinity cross sections of Miller, et al. (1970). Low-salinity Atlantic Water enters the Ionian Basin through the Strait of Sicily, but is well imbedded in the seasonal thermocline. This water mass tends to retard the formation of a strong negative velocity gradient above the DSC axis. The distribution and characteristics of Atlantic Water are described in detail by Moskalenko and Ovchinnikov (1965).

(U) Secondary sound channels frequently occur above and below the DSC axis. Those above the DSC axis generally are caused by perturbations in temperature structure at the base of the seasonal thermocline. Those below the DSC axis generally are separated from the axis by a sound velocity maximum that coincides with the LIW high-salinity core, and probably are caused by mixing in the LIW layer. Occasionally, one of the sound velocity minima below the LIW core is the absolute sound velocity minimum (i.e., the DSC axis). However, this situation is more common farther east in the Levantine Basin.

(U) Oceanic fronts have been observed in the central Ionian Sea during winter, spring, and summer by several investigators. Figure 7 summarizes approximate observed positions of these fronts. The average winter positions shown in figure 7 are from Ovchinnikov (1966) and are based on historical surface circulation patterns. In August 1966, a front with an east-west trend was found across most of the Ionian Sea (Levine and White, 1972). This front extended through the seasonal thermocline to depths of at least 100 m. During May 1971, a front oriented northwest-southeast was observed at the edge of the continental shelf southeast of Sicily. This front has been called the Maltese Front

UNCLASSIFIED

UNCLASSIFIED

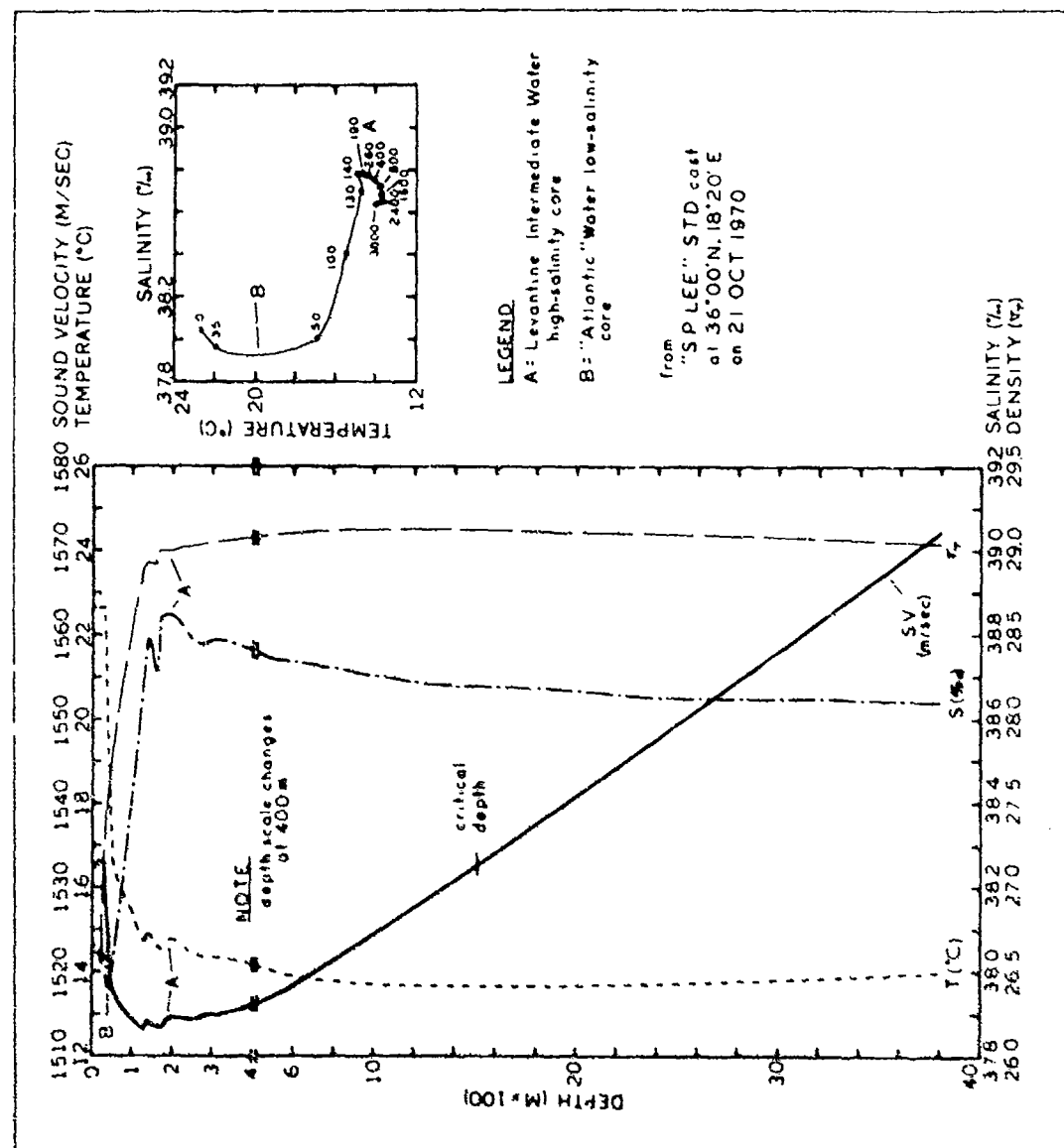


Figure 6. Historical Autumn Temperature-Salinity-Sound Velocity-Density Profiles and T-S Comparisons for Central Ionian Basin

UNCLASSIFIED

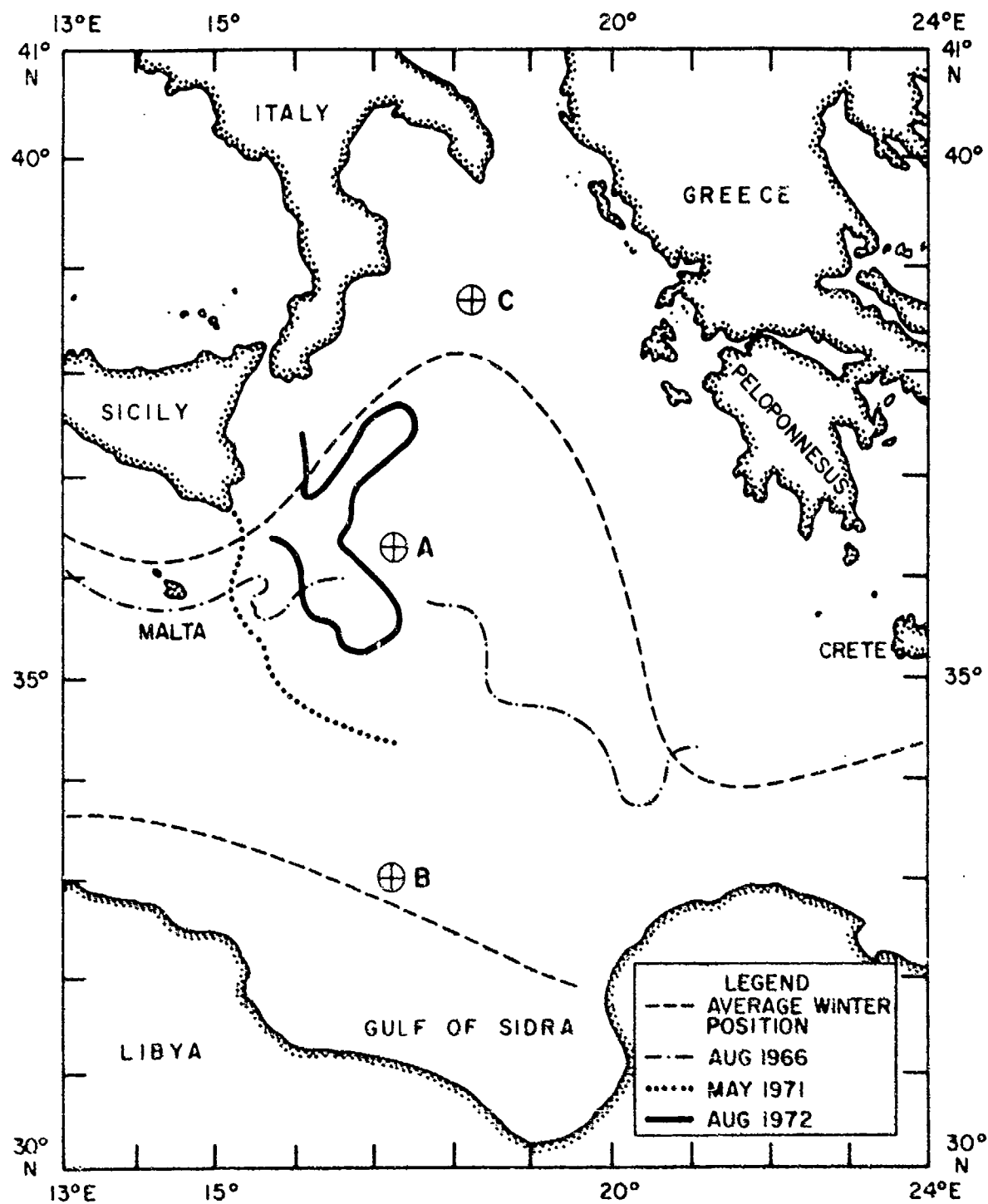


Figure 7. Positions of Oceanic Fronts Observed in Ionian Sea

UNCLASSIFIED

by Briscoe, et al. (1972) and other investigators. According to Johannessen, et al. (1971), the Maltese Front separates cool, less saline waters of the western Mediterranean Sea from warm, more saline waters of the Ionian and Levantine Basins and can extend to depths of 150 m. A near-surface front oriented similar to the Maltese Front was found in the vicinity of IOMEDEX point A during August 1972 as part of the Mediterranean TASSRAP Exercise (Maury Center for Ocean Science, 1972b). This front is described in detail by Anderson, et al. (1973). During IOMEDEX, the Maltese Front crossed the SANDS track east of Malta during 18-24 November (Miller, 1972). However, the density of SANDS XBT data was insufficient to chart the areal extent of this front. Limited SANDS data indicate that during IOMEDEX the Maltese Front separated water moving eastward from the Strait of Sicily from resident surface waters of the Ionian Sea.

(U) Another distinct oceanic front (convergence) has been reported just south of point B during winter by Ovchinnikov (1966). This front, shown in the lower part of figure 7, separates coastal waters in the Gulf of Sidra from surface waters to the north in the open Ionian Sea. According to Ovchinnikov, the position of this front is approximately the same in summer and winter.

(U) Prior to IOMEDEX, all available autumn historical sound velocity data were analyzed to predict probable critical depth (see glossary) at various receiver sites. However, this analysis was based on a very limited amount of September and October data, plus the November data collected by LEE during IMP. Figure 8 clearly shows the rapid changes in critical depth expected in the IOMEDEX area during autumn. During this season, critical depth frequently decreases very rapidly in response to cooling of the surface and near-surface layer. Since IOMEDEX measurements were made at the steepest slope on the annual critical depth curve, any deviation from average conditions (such as an early winter storm) could create anomalously shallow critical depths. Large temporal and spatial variations in critical depth are expected throughout the Ionian Sea during autumn owing to mixing caused by local storms and varying amounts of surface insolation. In much of the Ionian Sea, the DSC axis also decreases with time during autumn as a result of surface cooling and weakening of the seasonal thermocline.

#### NEAR-SURFACE THERMAL STRUCTURE

##### A. Sea Surface Temperature

(U) Sea surface temperature measurements during IOMEDEX were insufficient to map the areal extent of the Maltese Front, but were adequate to determine temperature changes over the duration of the exercise. Figures 9 and 10 show contours of surface temperature for the northern half of the IOMEDEX area during 8-14 and 23-26 November, respectively. Analysis areas for figures 9 and 10 are limited by

UNCLASSIFIED

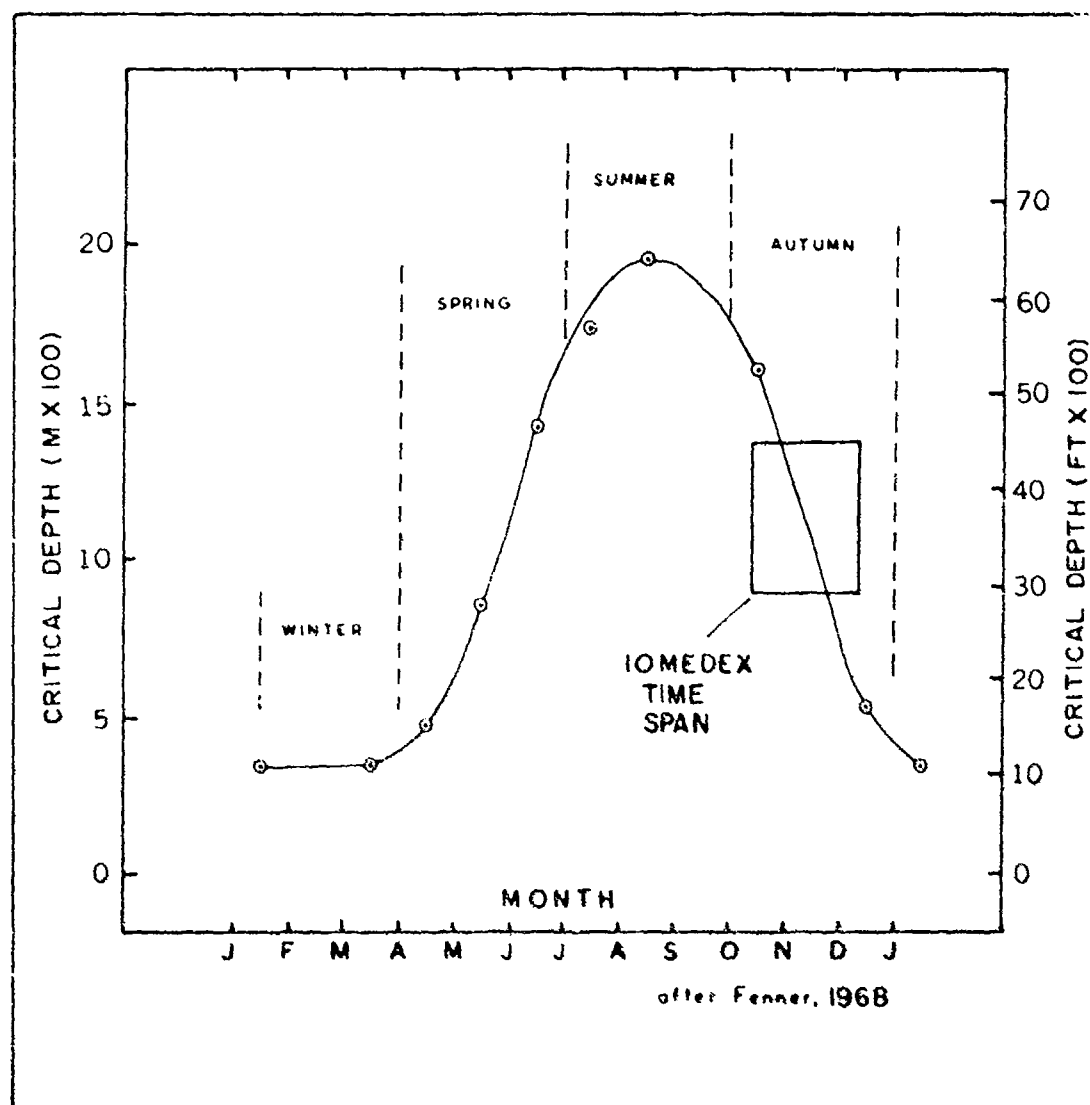


Figure 8. Average Monthly Critical Depths for Central and Southern Ionian Basin

UNCLASSIFIED

UNCLASSIFIED

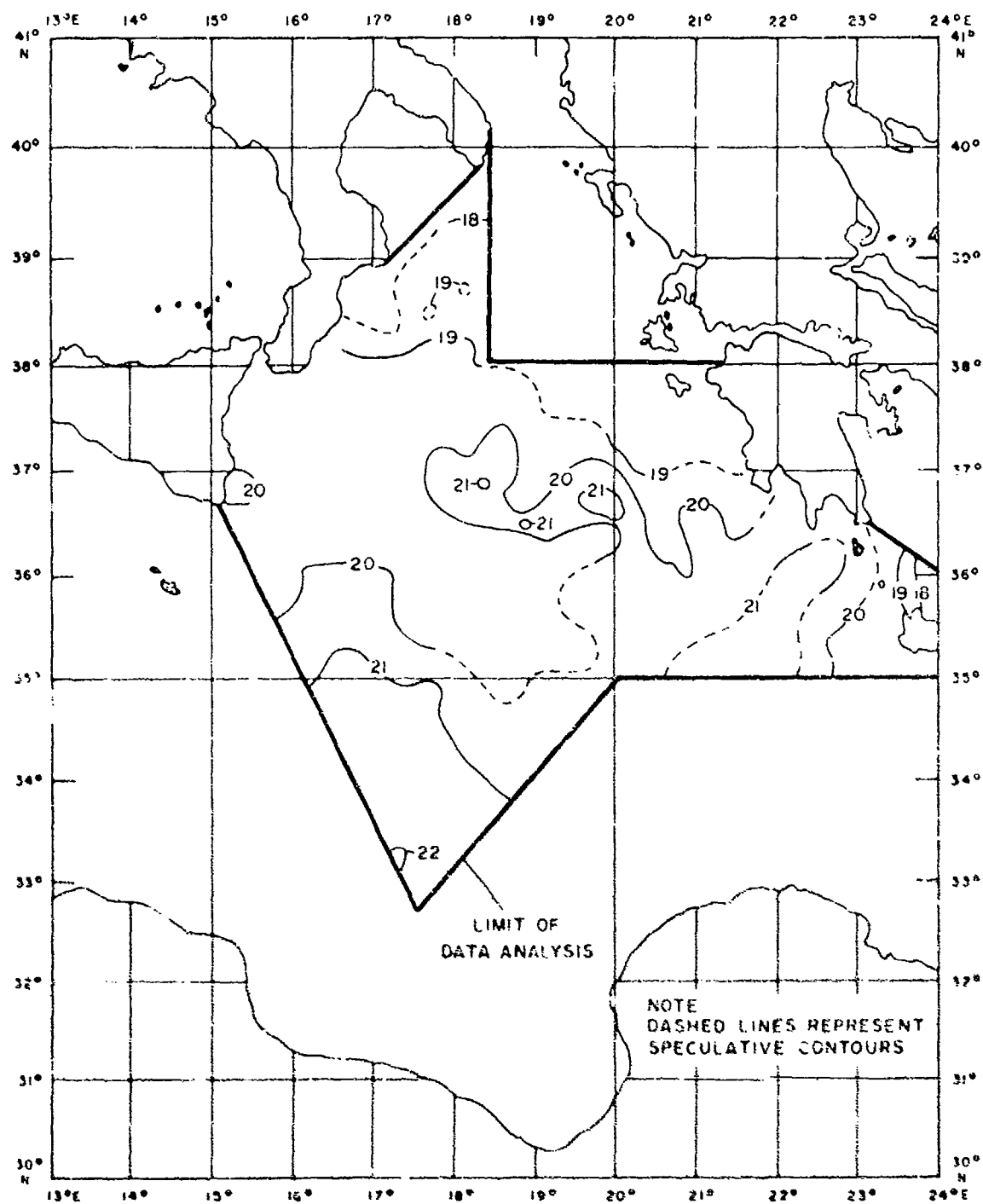


Figure 2. Sea Surface Temperature (C°) for 8-14 November



UNCLASSIFIED

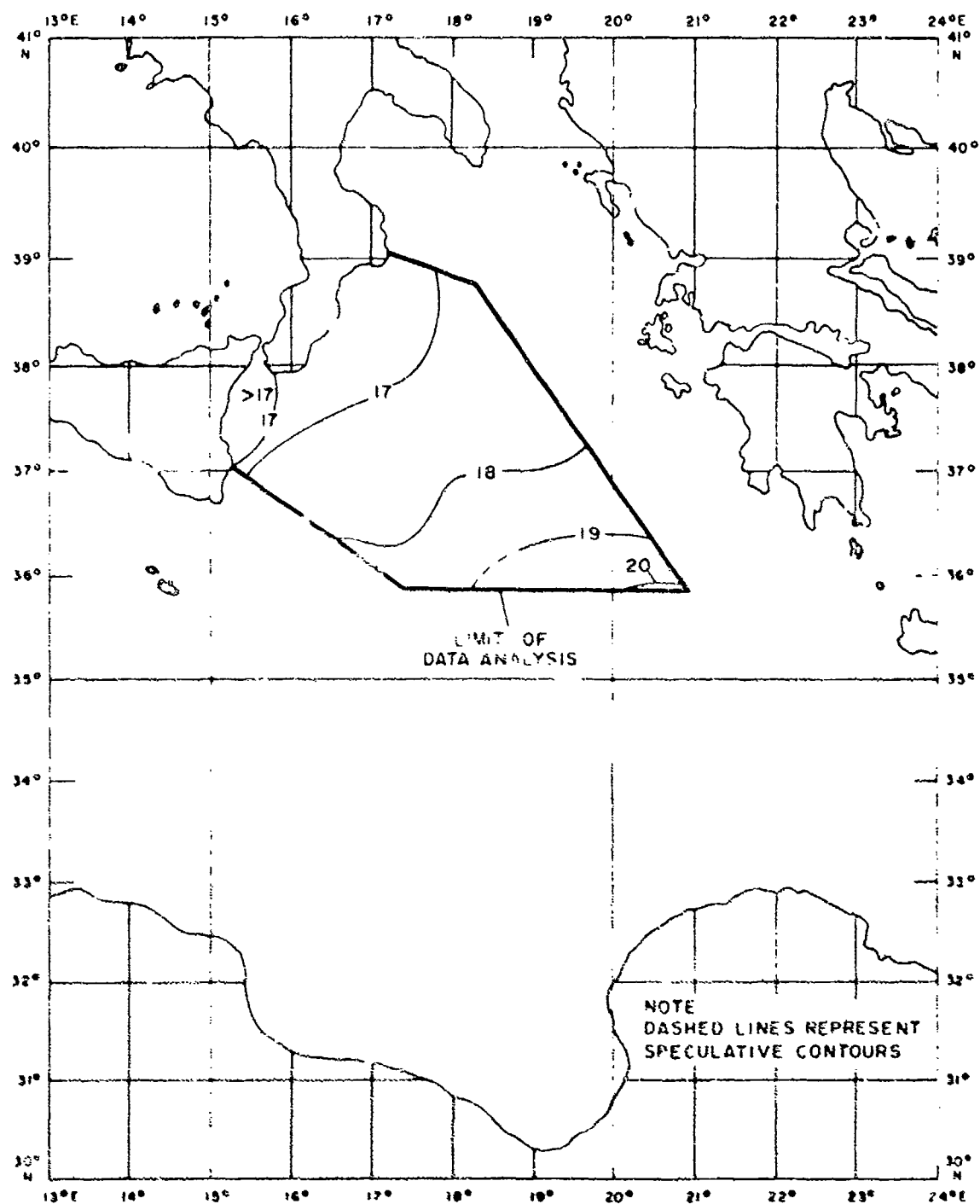


Figure 10. Sea Surface Temperature for 23-26 November

UNCLASSIFIED

## CONFIDENTIAL

temporal and spatial distribution of IOMEDEX data before and after the passage of a large depression on 19-23 November. Neither figure includes AXBT data owing to its questionable accuracy.

(C) Sea surface temperature in the central portion of the analysis area prior to the storm averaged about 20°C, and displayed a relatively stable series of isotherms. Temperature increased to about 22°C in the south, and values less than 18°C were observed in the northern and eastern extremities of the area. After passage of the depression, the isotherms were generally oriented northeast to southwest, perpendicular to the track followed by the storm. Near the northern edge of the analysis area, the storm apparently exerted its greatest effect; sea surface temperatures decreased by approximately 2°C. Along the southern edge, no significant changes in surface temperature were observed. The most noticeable effect of sea surface temperature decrease after the storm was a significant decrease in critical depth and increase in depth excess (see glossary). This increase in depth excess should have improved convergence zone propagation in the northern part of the IOMEDEX area.

### B. Mixed Layer Depth

(C) Figures 11 and 12 show mixed layer depth contours for the northern half of the IOMEDEX area during 11-14 and 23-26 November, respectively. XBT and AXBT data were used in constructing these figures. Figure 11 represents conditions prior to the passage of the large depression between 19 and 23 November. Figure 12 represents conditions after the passage of this cold front. Over the northern Ionian Sea as a whole, layer depths were 10 to 30 m deeper after the storm, and the depth of the mixed layer varied more than 50 m in the northwestern Ionian Sea and southwest of Peloponnesus. Before the storm, such variability was confined to the latter region, and layer depths were much more uniform throughout the northern Ionian Sea. The unusually deep mixed layers (greater than 100 m) southwest of Peloponnesus both before and after the storm were observed from several platforms and on XBT and AXBT traces. This anomaly may be a permanent feature during autumn. The variability in mixed layer depth before and after the storm probably has significant effects on surface duct echo ranging. However, some surface duct propagation appears possible everywhere in the IOMEDEX area.

## SOUND VELOCITY STRUCTURE

### A. Temporal Variability at Points A, B, and C

(C) Figure 13 shows 16 sound velocity profiles collected at point A plotted as a time series. Despite the large time gaps, this figure shows a significant decrease in critical depth from about 1300 m on 31 October to about 1100 m on 6-7 November when acoustic measurements began. During the acoustic experiments, critical depth decreased an

UNCLASSIFIED

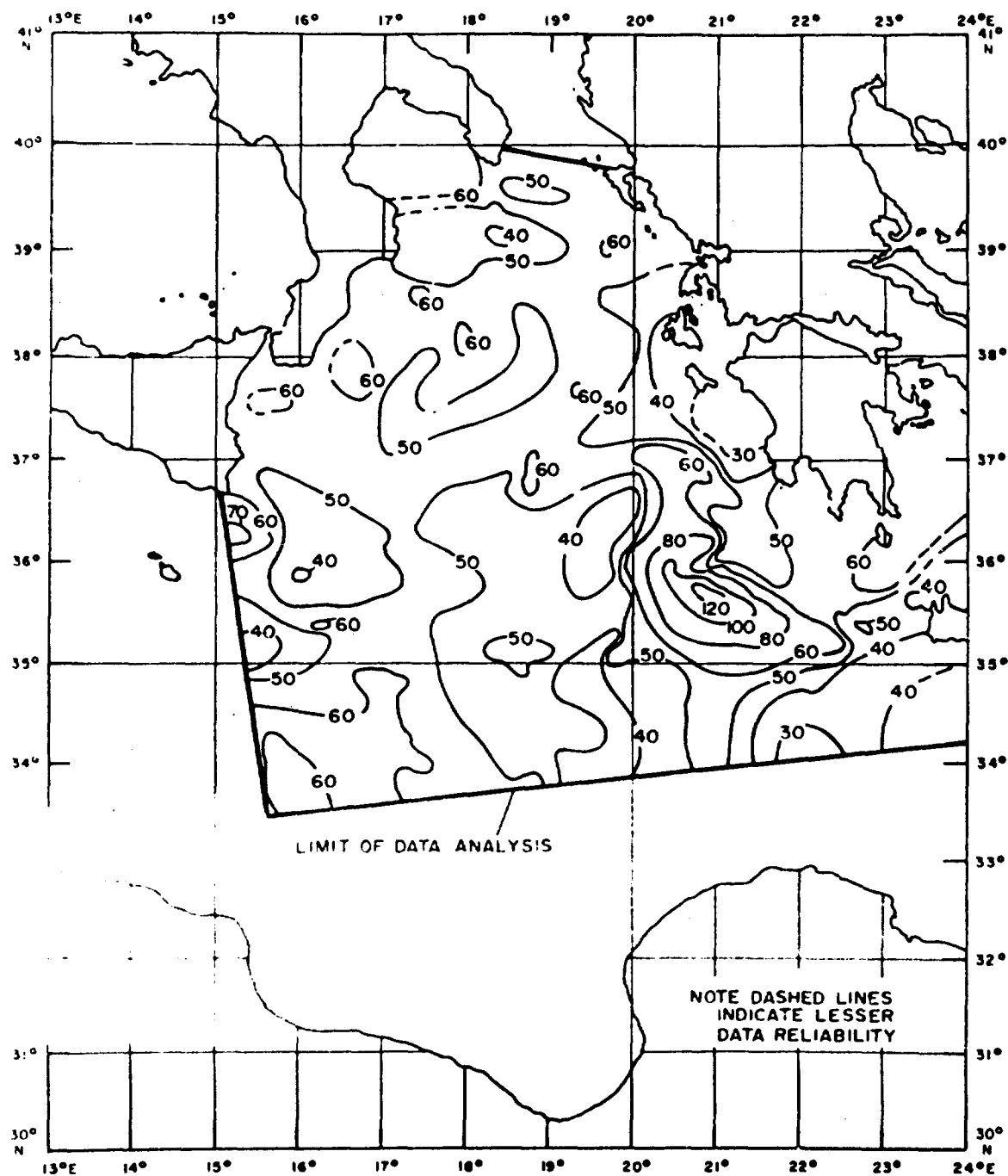


Figure 11. Mixed Layer Depth (m) for 11-14 November

UNCLASSIFIED

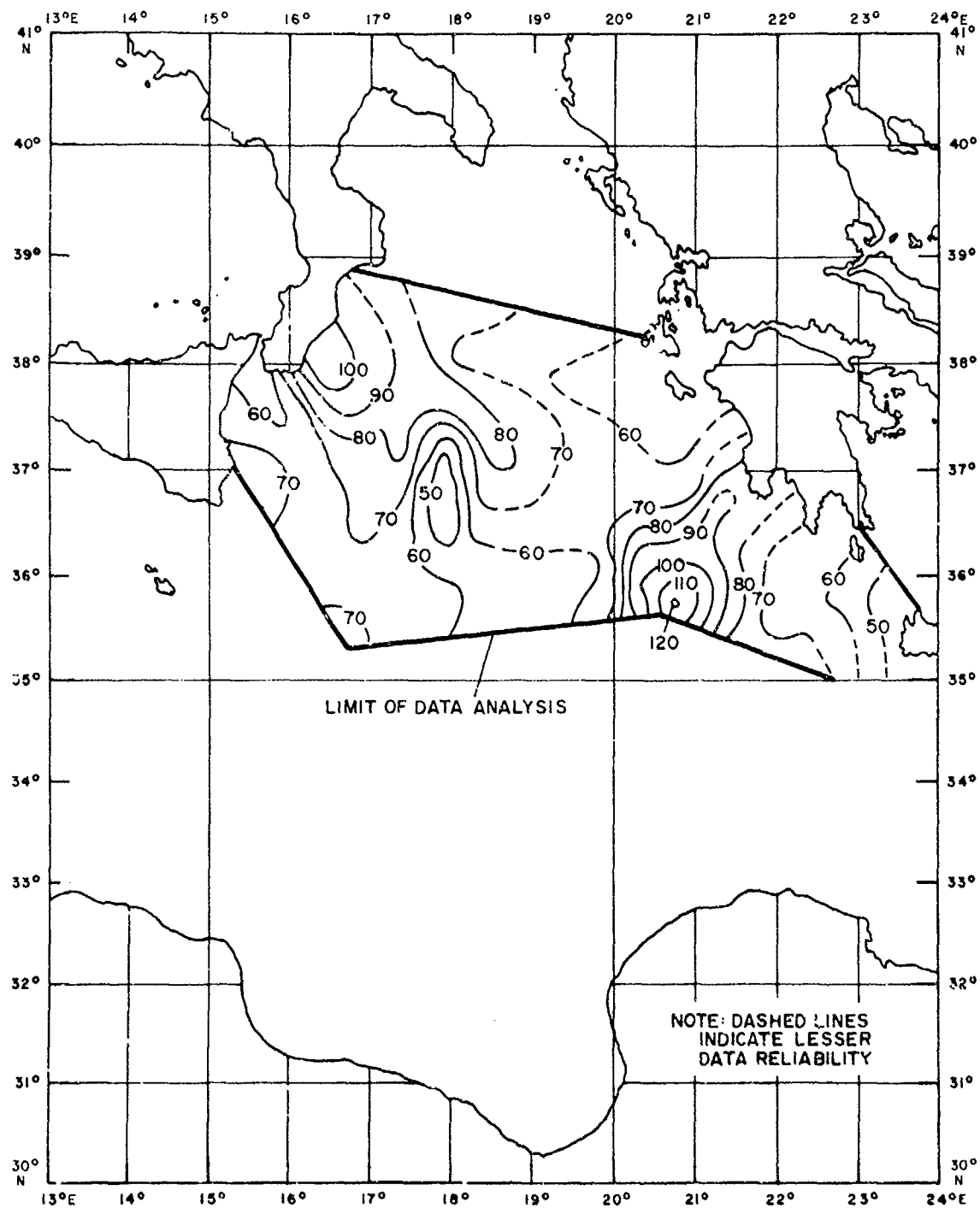
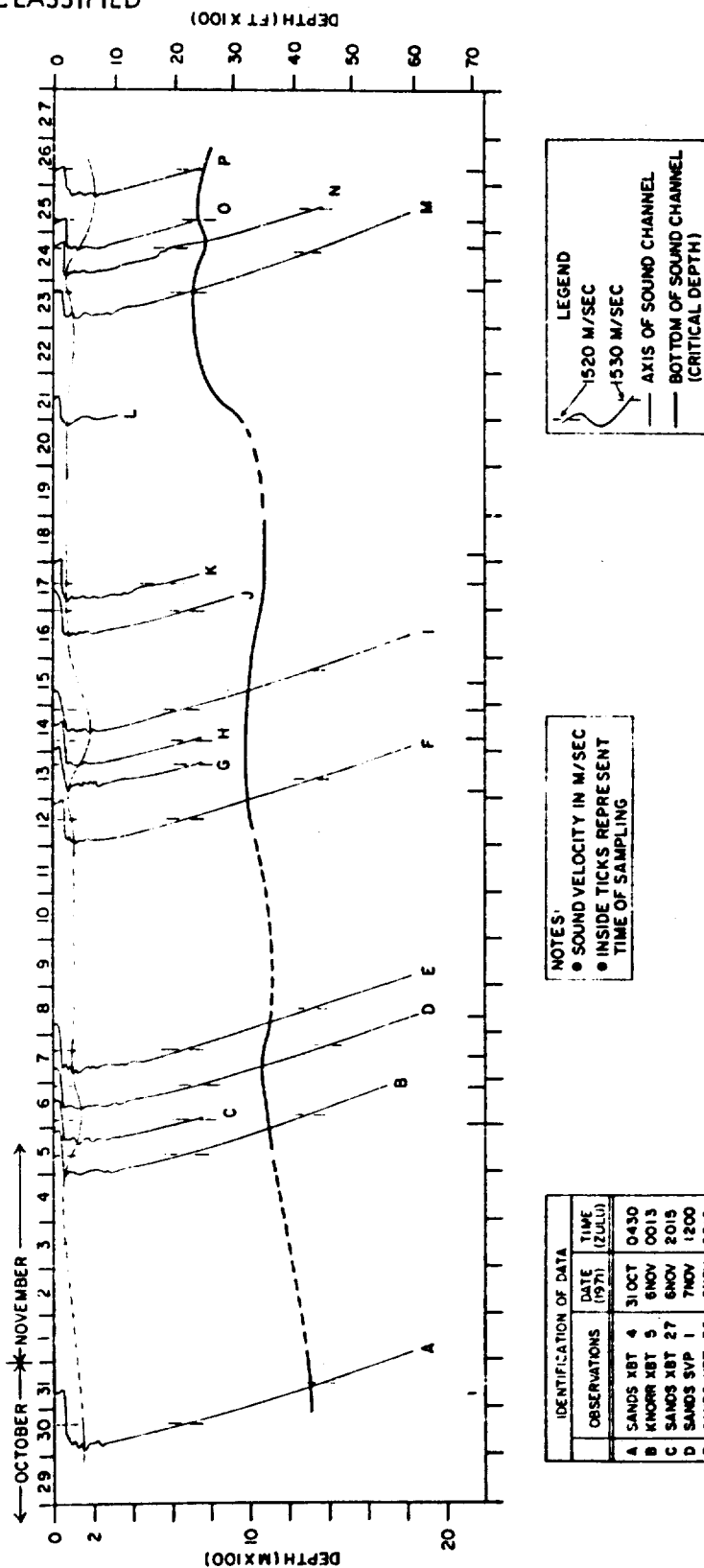


Figure 12. Mixed Layer Depth (m) for 23-26 November

UNCLASSIFIED



IDENTIFICATION OF DATA		
OBSERVATIONS	DATE (1971)	TIME (ZULU)
A SANDS XBT 4	31 OCT	0430
B KNORR XBT 5	6 NOV	0013
C SANDS XBT 27	6 NOV	2015
D SANDS SVP 1	7 NOV	1200
E SANDS XBT 36	8 NOV	0810
F NORTH SEAL XBT 35	13 NOV	0230
G SANDS XBT 78	14 NOV	0643
H SANDS XBT 83	14 NOV	2100
I SANDS XBT 86	15 NOV	1100
J SANDS XBT 93	17 NOV	1330
K SANDS XBT 97	18 NOV	0400
L VP-8 XBT 122	21 NOV	0909
M SANDS XBT 138	23 NOV	1905
N SANDS XBT 142	24 NOV	1630
O NORTH SEAL XBT 116	25 NOV	0517
P KNORR XBT 43	26 NOV	0710

Figure 13. Time-Series Plot of Sound Velocity at Point A (31 Oct-26 Nov)

CONFIDENTIAL

additional 350 m to a level of about 750 m on 23-24 November. The most rapid decrease occurred between 19 and 23 November when a large depression passed near point A. Critical depths at point A approximated the historical average at the beginning of the acoustic experiments (compare with figure 8), but were several hundred meters less than expected for mid-November. This anomalous situation probably was caused by surface and near-surface cooling associated with the storm. The corrected bottom depth at point A is approximately 3300 m. Therefore, depth excess was adequate for convergence zone propagation from a near-surface source throughout IOMEDEX.

(C) The DSC axis at point A varied between about 50 and 200 m during the exercise, and displayed significant short-term variations from a mean value of about 150 m. The nearly 100-m changes in the depth of the DSC axis on 6-7, 13-18 and 23-26 November were caused either by internal waves or the proximity of the Maltese Front. The Maltese Front was observed near point A between 18 and 24 November (Miller, 1972). The overall sound velocity structure in the upper 300 m of the water column at point A was rather complex probably because of mixing in the high-salinity LIW layer. Multiple sound velocity minima found throughout the exercise at point A resulted in short-term secondary or depressed sound channels. Such transient channels can provide good detection of a target located at the depth of the channel, but only for short periods and at limited ranges.

(C) Figure 14 shows five sound velocity profiles collected at point B plotted as a time series. Although data were very limited at this point, figure 14 shows a decrease in critical depth from about 1600 m on 1 November to about 1300 m on 20 November. Generally, critical depths were 200 to 400 m deeper at point B than at point A due to latitudinal effects, and were several hundred meters deeper than expected in the southern Ionian Basin (see figure 8). However, depth excess at point B was always adequate for convergence zone propagation from a near-surface source during IOMEDEX. The DSC axis depth decreased by about 200 m at point B during the exercise as a result of autumn cooling and/or varying concentrations of LIW. Multiple sound channels were not as common at point B as they were at point A owing to smaller concentrations of LIW in the southern Ionian Basin.

(C) Figure 15 shows 10 sound velocity profiles collected at point C plotted as a time series. Again, these data are very limited, but do show a decrease in critical depth from about 1000 m on 7 November to about 500 m on 25 November. Critical depths at point C during IOMEDEX were 100 to 200 m less than those at point A (figure 13) and 300 to 500 m shallower than those at point B (figure 14) because of cooler near-surface temperatures in the northern Ionian Sea. Depth excess at point C was more than adequate for convergence zone propagation from a near-surface source throughout the exercise. The DSC axis varied between about 80 and 160 m and averaged about 100 m. Multiple sound channels occurred at point C throughout the exercise, but were not as well-developed as those at point A owing to lower concentrations of LIW.

UNCLASSIFIED

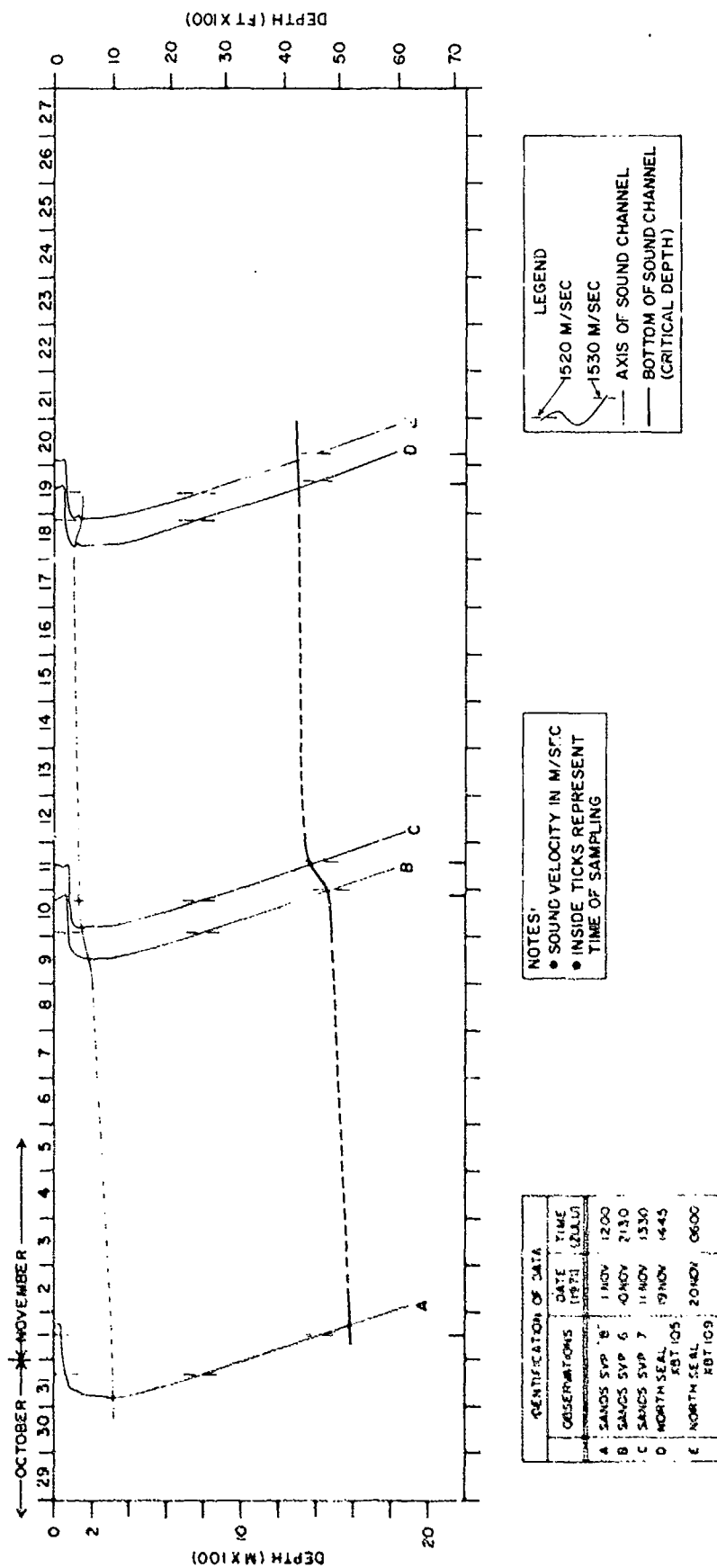


Figure 14. Time-Series Plot of Sound Velocity at Point B (1-21 Nov)

UNCLASSIFIED

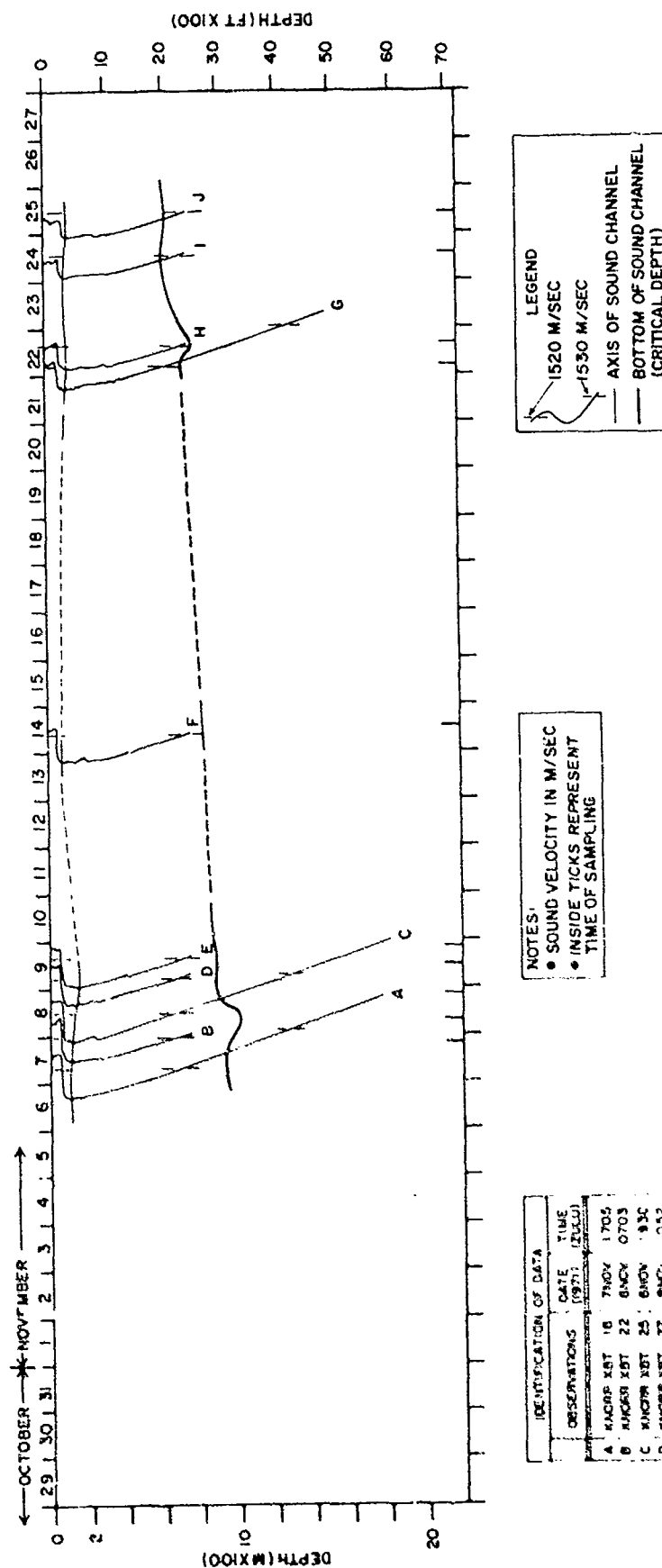


Figure 15. Time-Series Plot of Sound Velocity at Point C (7-25 Nov)

UNCLASSIFIED



CONFIDENTIAL

(C) In summary, relatively shallow critical depths found at points A, B, and C allowed uninterrupted convergence zone propagation from a near-surface source at all times during IOMEDX. Furthermore, the persistent decrease in critical depth with time at all three points improved convergence zone propagation throughout the Ionian Sea during the exercise. The DSC axis varied between about 50 and 300 m at the three points and averaged about 150 m. This agrees with historical averages (Brockhurst, 1960, and Fenner, 1968). Multiple sound channels occurred at all three points but were better developed in the central Ionian Basin (point A) in association with greater LIW concentrations.

B. Sound Velocity Structure Between Points A and C

(C) Figure 16 shows 12 sound velocity profiles along a north-northwestward track from point A to point C. Data used in this figure were collected between 7 and 15 November when the majority of acoustic receivers were operational at points A and C. Figure 17 is a contoured cross section of the data given in figure 16. A bathymetric profile from KNORR data is plotted in both figures.

(U) Surface sound velocities along track A-C varied from 1526.5 m/sec at the southern end of the track to 1522.1 m/sec near point C. A sporadic mixed layer occurred to depths of between 40 and 60 m on most profiles, and was best developed in the north. The DSC axis varied between about 90 and 200 m along track A-C, while the sound velocity at the DSC axis varied between 1512.0 and 1516.1 m/sec. The DSC axis was deepest about 80 nm from point A (NORTH SEAL XBT 69), and sound velocity at the DSC axis was greatest about 50 nm from point A (NORTH SEAL XBT 72). These maxima roughly correspond to a preferential flow of LIW extending westward from the Peloponnesian coast into the Ionian Sea between about 37° and 38°N (Moskelenko and Ovchinnikov, 1965). The closure of the 1515-m/sec isopleths and the doming of the 1516-m/sec isopleth about 50 nm from point A (figure 17) may indicate the Maltese Front that separates cooler, less saline waters west of the track from warmer, more saline waters east of the track. Secondary sound channels occurred above and below the DSC axis, particularly along the southern half of the track. The former were caused by temperature perturbations at the base of the permanent thermocline, the latter by mixing in the high-salinity LIW layer.

(C) Critical depth generally decreased northward from greater than 1000 m near point A to about 900 m at point C, and closely followed the 1525 m/sec sound velocity isopleth (figure 17). Critical depth varied significantly between about 30 and 60 nm from point A. In this region, critical depth fluctuated about 250 m over distances of about 15 nm. This fluctuation may be related to a meander in the Maltese Front. Depth excess along track A-C was never less than 1400 m, allowing unimpeded convergence zone propagation from a near-surface source.

UNCLASSIFIED

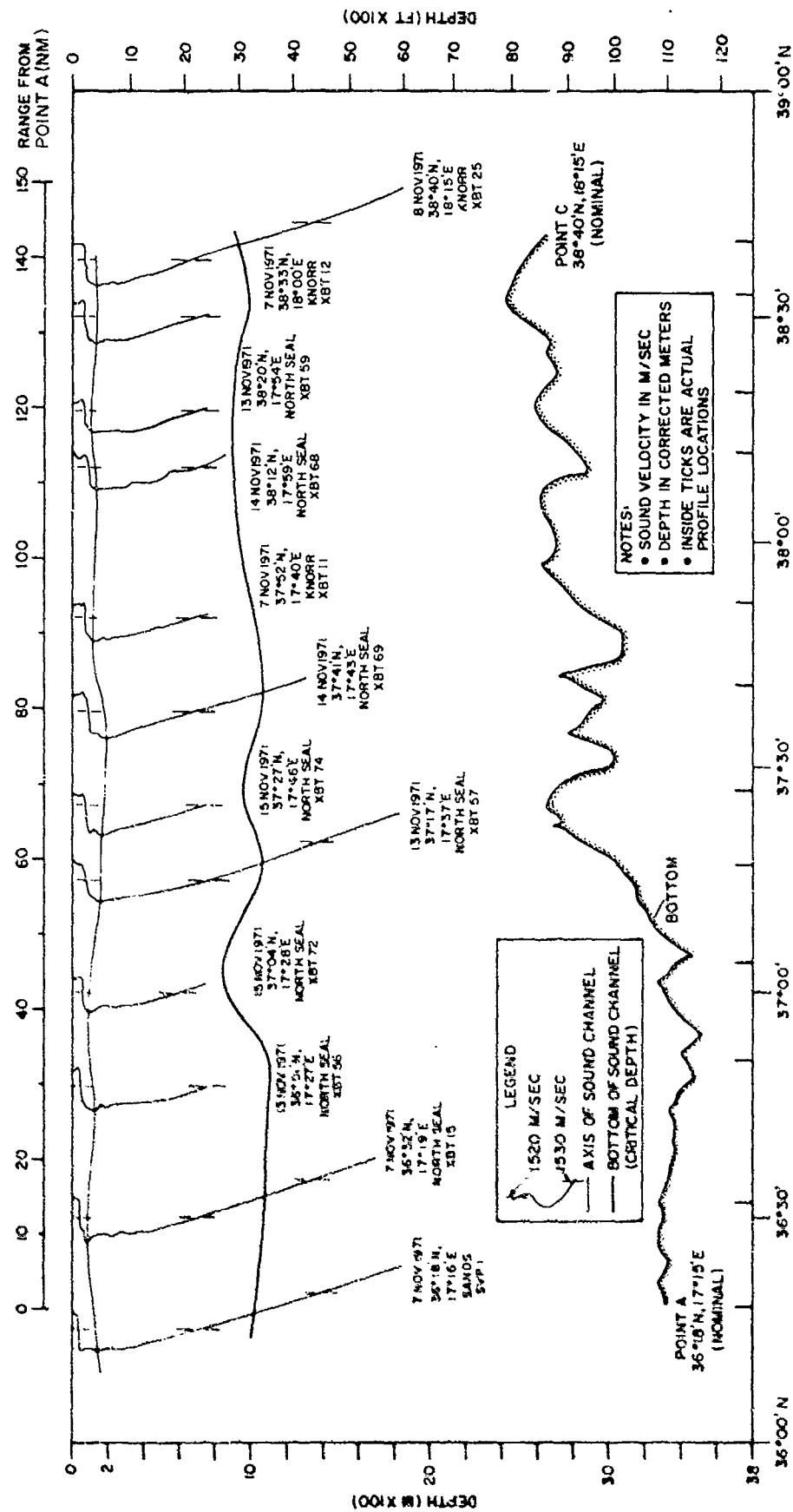


Figure 16. Sound Velocity Profiles from Point A to Point C (7-15 Nov)

UNCLASSIFIED

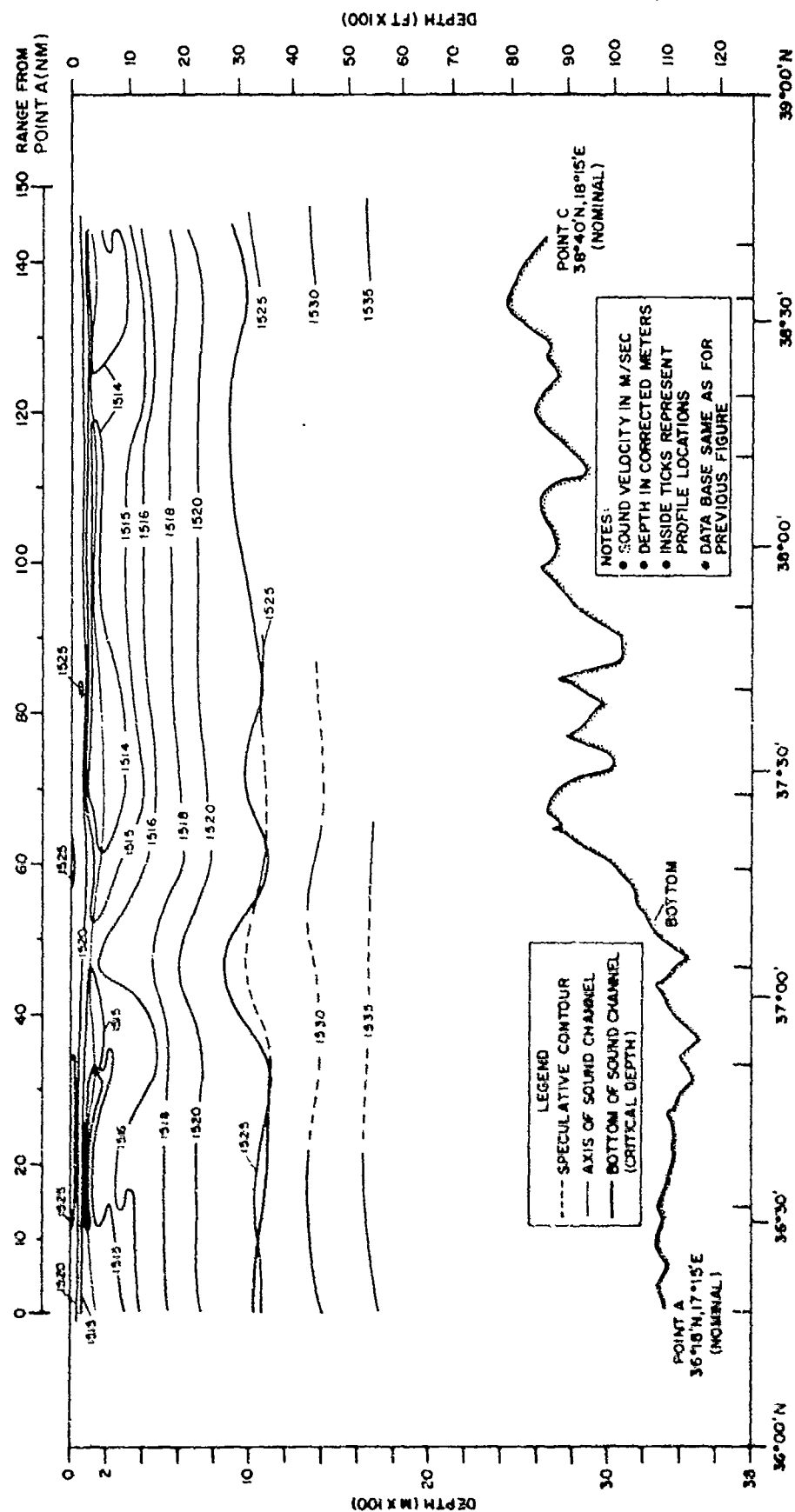


Figure 17. Sound Velocity Cross Section from Point A to Point C (7-15 Nov)

UNCLASSIFIED

UNCLASSIFIED

### C. Sound Velocity Structure Between Point A and Point B

(U) Figure 18 shows 16 sound velocity profiles along a track due north from point B to point A. All data used in this figure were collected between 10 and 20 November. Figure 19 is a contoured cross section of the same data displayed in figure 18. A bathymetric profile from SANDS data is plotted in both figures.

(U) Surface sound velocities along track B-A varied from 1530.8 m/sec in the south to 1522.4 m/sec near point A. A mixed layer occurred on most of the profiles at depths between about 30 and 80 m. The negative sound velocity gradient below the mixed layer was stronger along track B-A than along track A-C (figure 16), because of less autumnal cooling in the southern Ionian Basin. The DSC axis varied from about 150 m at point B to greater than 300 m at a range of 25 nm, and then remained at about 300 m for about 70 nm. North of about 35°N (120 nm from point B), the DSC axis fluctuated between about 90 and 200 m, a situation similar to that observed along track A-C. Sound velocity at the DSC axis varied from 1511.9 m/sec at point A to 1517.5 m/sec about 80 nm from point B (NORTH SEAL XBT 102). Sound velocities at the DSC axis were generally less than 1515 m/sec near point B and at points more than 120 nm northward. At ranges between 20 and 120 nm, the high values of axial depth and sound velocity probably were caused by the preferential flow of high salinity LIW across the Ionian Basin described by Wüst (1961).

(U) Secondary sound channels occurred above and below the DSC axis along much of track B-A. At ranges between 20 and 120 nm from point B, these channels primarily occurred above the DSC axis, and probably were caused by the presence of high-salinity LIW. However, north of about 35°N, secondary sound channels above the DSC axis were caused by temperature perturbations at the base of the permanent thermocline. In this same region, secondary sound channels below the DSC axis were separated from the DSC axis by a sound velocity maximum that coincided with the LIW high-salinity core. The near-closures of the 1518-m/sec isopleth at positions about 60 and 110 nm north of point B (figure 19) apparently delineate the northern and southern limits of the major LIW core in the central Ionian Basin. The domed structures in the 1516-m/sec isopleth (at about 170 nm) and in the 1518- and 1520-m/sec isopleths (at about 110 nm) may indicate meanders of the Maltese Front crossing track B-A. The Maltese Front was observed during IOMEDEX by Miller (1972) at about 36°N, just south of point A. However, high-salinity LIW had a much more pronounced influence on the DSC along track B-A than did the meandering Maltese Front.

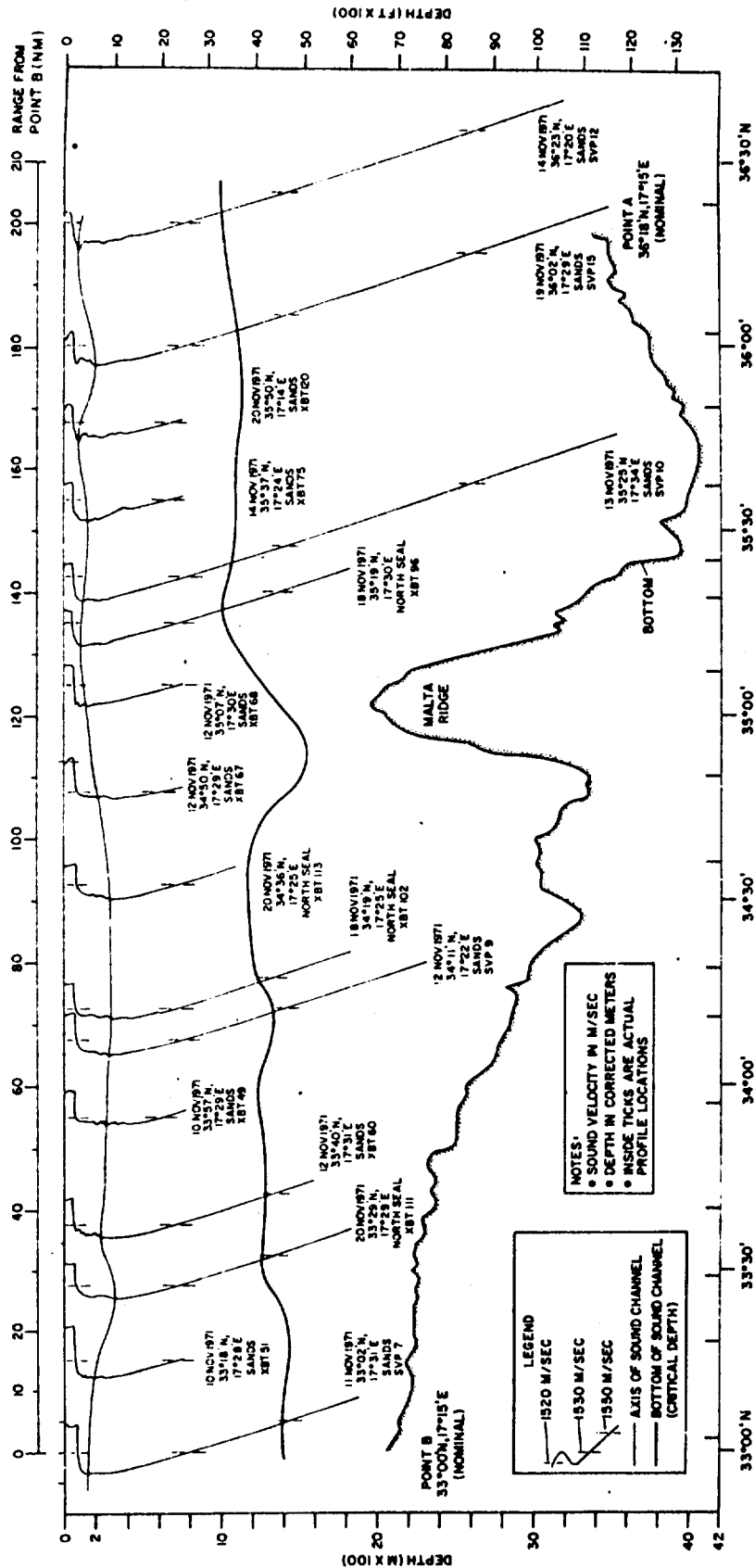


Figure 18. Sound Velocity Profiles from Point B to Point A (10-20 Nov)

UNCLASSIFIED

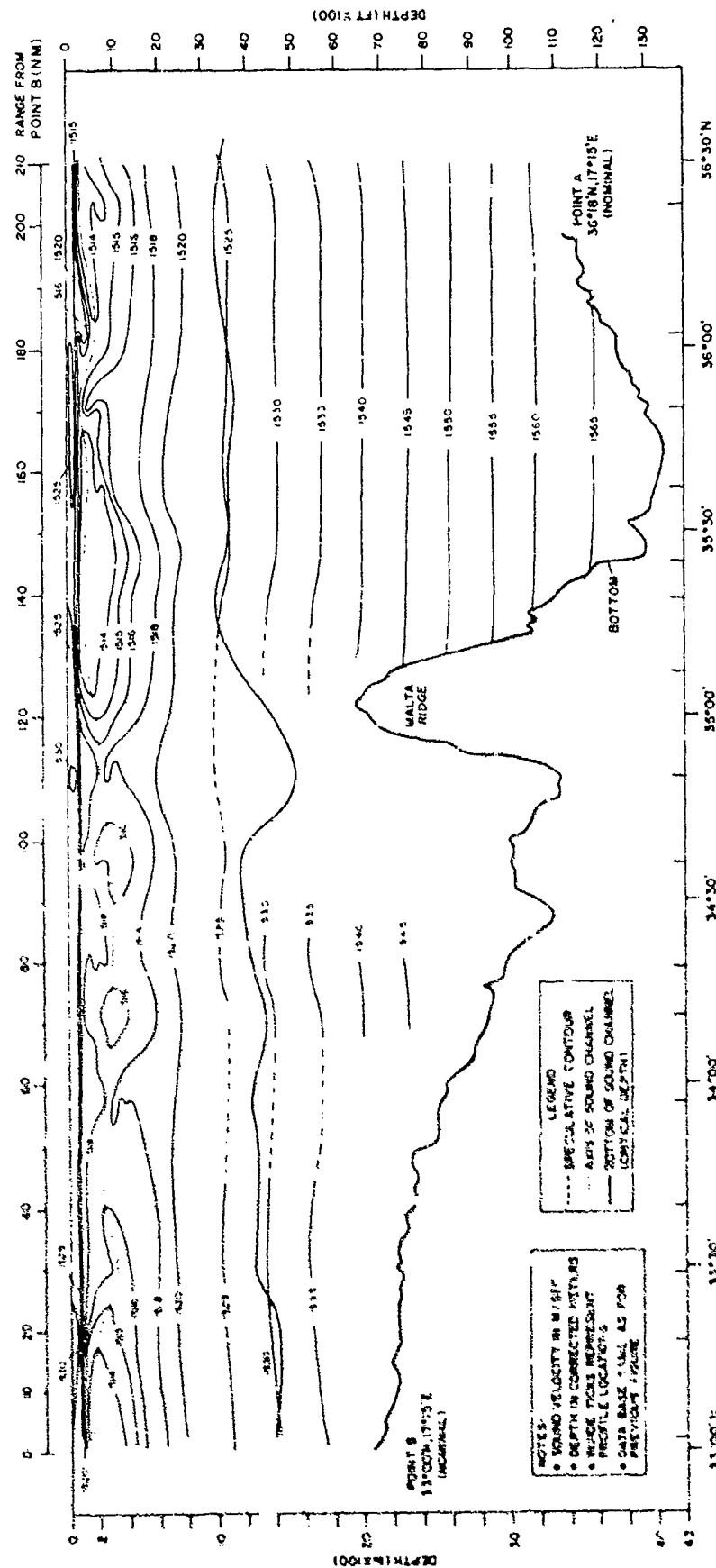


Figure 10. Sound Velocity Cross Section from Point B to Point A (10-20 Nov)

CONFIDENTIAL

(U) Critical depth generally decreased northward from greater than 1400 m at point B to about 1000 m at point A and significantly varied at ranges between about 100 and 130 nm. At these ranges, critical depth rapidly increased about 400 m and then decreased about 500 m. This anomalous situation probably was caused by meanders of Maltese Front. In this region, the Maltese Front separates cooler, less saline water of the northern and central Ionian Sea (shallow critical depths) from warmer, more saline waters to the south (deep critical depths). The front probably crossed track B-A at about 34°45'N. This position corresponds well with the position where the Maltese Front was observed to breakup during May 1971 (see figure 7).

(C) At point B, relatively deep critical depths and the relatively shallow bathymetry of the continental slope off Libya reduced depth excess to less than 600 m. This is the minimum depth excess observed at any IOMEDEX reference point. Depth excess was even less (about 400 m) where track B-A crosses the Malta Ridge. A depth excess of 400 m is considered marginal for reliable convergence zone propagation from a near-surface source. However, the 1960-m depth of the Malta Ridge shown in figures 18 and 19 probably represents its shallowest extent. East and west of the point where track B-A crosses the ridge the bottom is several hundred meters deeper. Since there are no other significant topographic intrusions into the DSC, reliable convergence zone propagation should have been possible along most of track B-A during IOMEDEX.

CURRENT MEASUREMENTS

(U) During IOMEDEX, NAVOCEANO implanted and recovered two taut-line, self-contained current measuring arrays. Array 1 was implanted near point A (36°16'N, 17°19'E) in 3350 m (11,000 ft) of water from 6 to 26 November. Array 2 was implanted near point C (38°39'N, 18°16'E) in 2700 m (8860 ft) of water from 8 to 25 November. Configurations of the vertical current meter arrays are shown in figures 20 and 21. A data summary for each of the Richardson-type current meters (Geodyne Model A-101-1) is given in table 2.

(U) After recovery, current meter film was developed for high density contrast and reduced to a computer compatible format. Data from each meter were processed to produce a listing of hourly current speed averages (in 5 cm/sec intervals) versus direction referenced to magnetic north in (15 degree intervals). Current data are presented in appendix B. These tabulations represent only that part of each current meter data record which was computer processed, not the total available record (as shown in table 2).

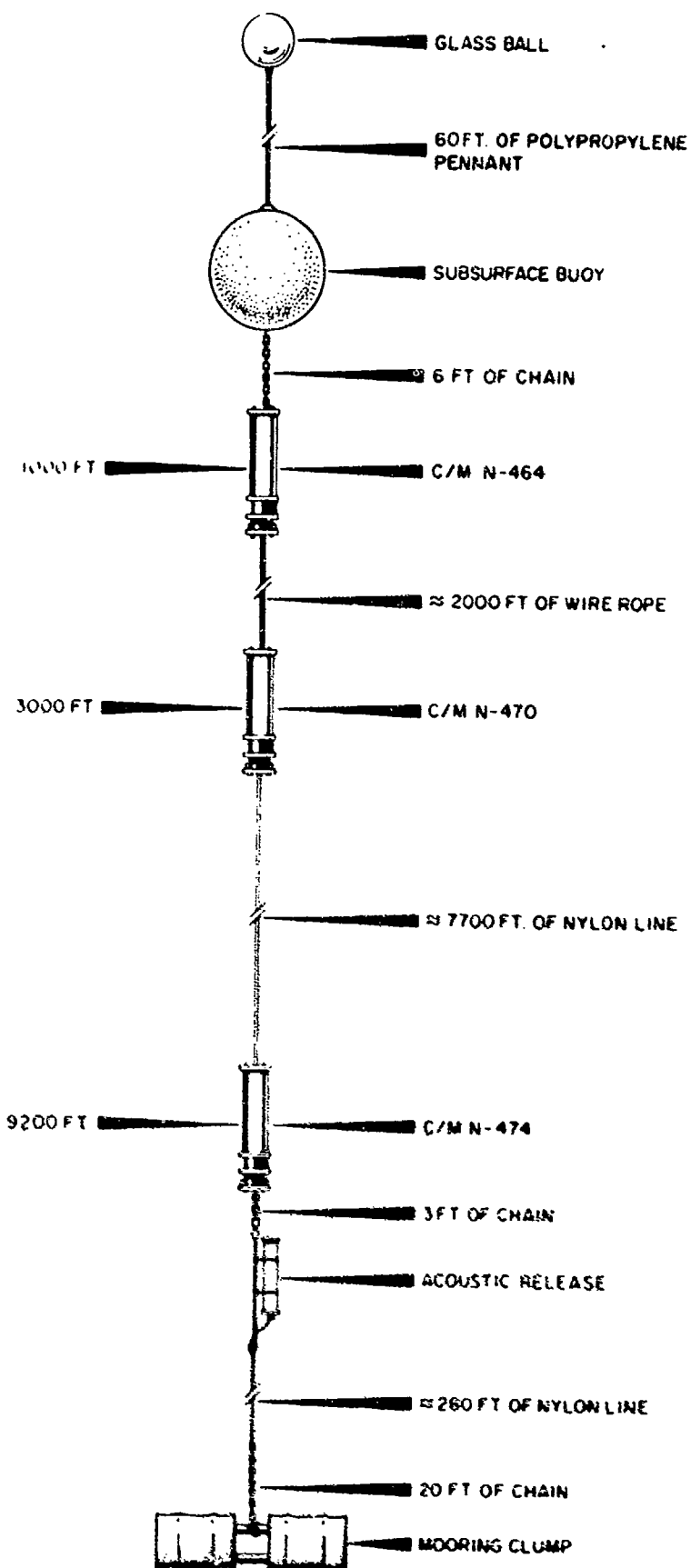


Figure 20. Current Meter Array 1, Point A - 36°16'N, 17°19'W



UNCLASSIFIED

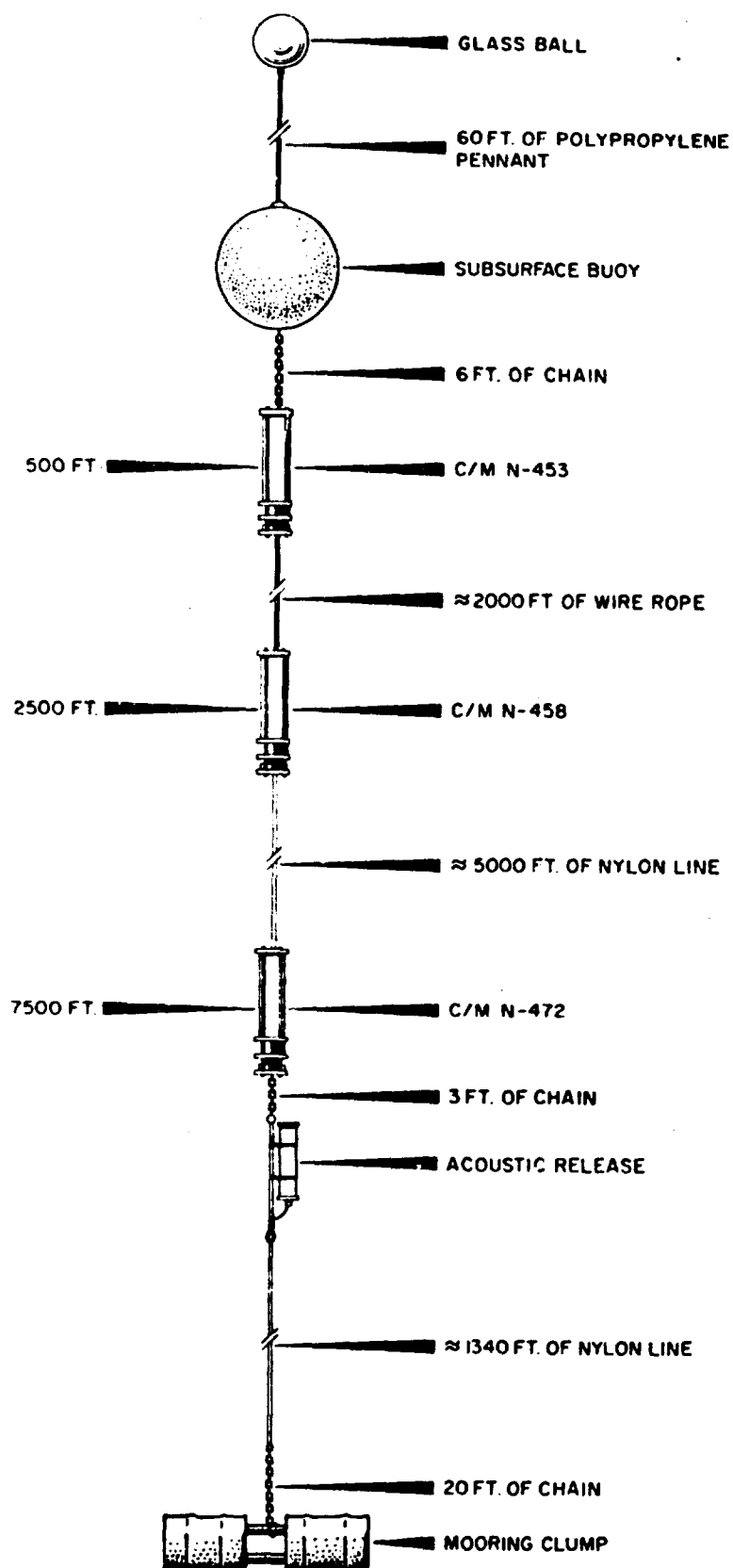


Figure 21. Current Meter Array 2, Point C - 38°59'N, 18,16'E

UNCLASSIFIED

UNCLASSIFIED

Current Meter	Meter Depth	Meter Start Time	Array Moored	Release Fired	Meter Stop Time	Sampling Interval	Record Length	No. Frames (calculated)	No. Frames On Mag Tape
Array 1, Point A 36°16'N, 17°19'E Depth 3350 m (11000 ft)									
N-464	305 m (1000 ft)	6 Nov 0125	6 Nov 0450	26 Nov 0800	26 Nov 1335	10 min	492 hr 10 min	2953	1722
N-470	914 m (3000 ft)	6 Nov 0125	6 Nov 0450	26 Nov 0800	26 Nov 1350	10 min	492 hr 25 min	2954	2954
N-474	2804 m (9200 ft)	6 Nov 0125	6 Nov 0450	26 Nov 0800	26 Nov 1410	10 min	492 hr 45 min	2956	2952
Array 2, Point C 38°39'N, 18°16'E Depth 2700 m (8860 ft)									
N-453	152 m ( 500 ft)	8 Nov 0935	8 Nov 1210	25 Nov 1040	25 Nov 1500	10 min	413 hr 25 min	2480	2955
N-458	762 m (2500 ft)	8 Nov 0935	8 Nov 1210	25 Nov 1040	25 Nov 1455	10 min	413 hr 20 min	2480	2478
N-472	2286 m (7500 ft)	8 Nov 0935	8 Nov 1210	25 Nov 1040	25 Nov 1500	10 min	413 hr 25 min	2480	2480

Note: All times GMT (Zulu)

Table 2. Summary of IOMEDX Current Meter Data

UNCLASSIFIED

UNCLASSIFIED

(U) Near point A, the current is predominantly north-northeasterly with an average speed of 6.9 cm/sec (0.13 kn) at a depth of 305 m, and 5 cm/sec (0.10 kn) at 914 m. The current at 2804 m is easterly with a maximum speed of 5 cm/sec (0.10 kn).

(U) Near point C, the current at a depth of 152 m is east-northeasterly with an average speed of 30 cm/sec (0.58 kn). At a depth of 762 m, the current is easterly with an average speed of 6.8 cm/sec (0.14 kn). At a depth of 2286 m, the current is also easterly with a maximum speed of 5 cm/sec (0.10 kn).

#### SEA, SWELL, AND WEATHER OBSERVATIONS

(U) Figure 22 summarizes wind force, wind direction, sea state, and swell height observations made during IOMEDEX by SANDS, NORTH SEAL, and KNORR. This figure does not provide exact conditions at any given location in the Ionian Sea, since many of the individual data points are based on an average of three observations made by different ships at disparate locations. However, this figure accurately depicts predominant conditions in the IOMEDEX area on the dates indicated. In general, the severity of storms passing through the Ionian Sea increased during the course of IOMEDEX. Wind speeds were high on 9, 13, 21, and 22 November and low on 4, 11, and 16 November. High wind speeds observed after 19 November mark the passage of the large depression that had significant effects on near-surface oceanographic conditions. In enclosed basins like the Ionian Sea, sea state and swell height closely follow local wind conditions. Therefore, most rough weather during IOMEDEX persisted only as long as the storm that caused it.

(U) Between 1 and 4 November, a high-pressure center with several cells over western Europe dominated the wind field and caused weak northerly flows over the Ionian Sea. By 1200Z on 5 November, a well-developed frontal system had approached the European coast. The high-pressure center then shifted southward to North Africa, and the Ionian Sea gradually came under the influence of the warm sector of the advancing frontal system. This system gradually became diffuse as the front became stationary over Italy.

(U) By 9 November, a well-developed low was approaching, and again the exercise area was under the influence of a warm sector. By 10 November, a well-developed low-pressure center over the western Mediterranean Sea dominated the weather in the Ionian Sea. Cold frontal passage over Sicily occurred at about 0600Z, 11 November. However, the flow was still northward over much of the exercise area. By 14 November, the low-pressure center shifted over the Ionian Sea, causing a somewhat diffuse weather situation. At this time, the dominant weather feature was a high over the eastern Atlantic with an intense low over the Baltic Sea.

UNCLASSIFIED

UNCLASSIFIED

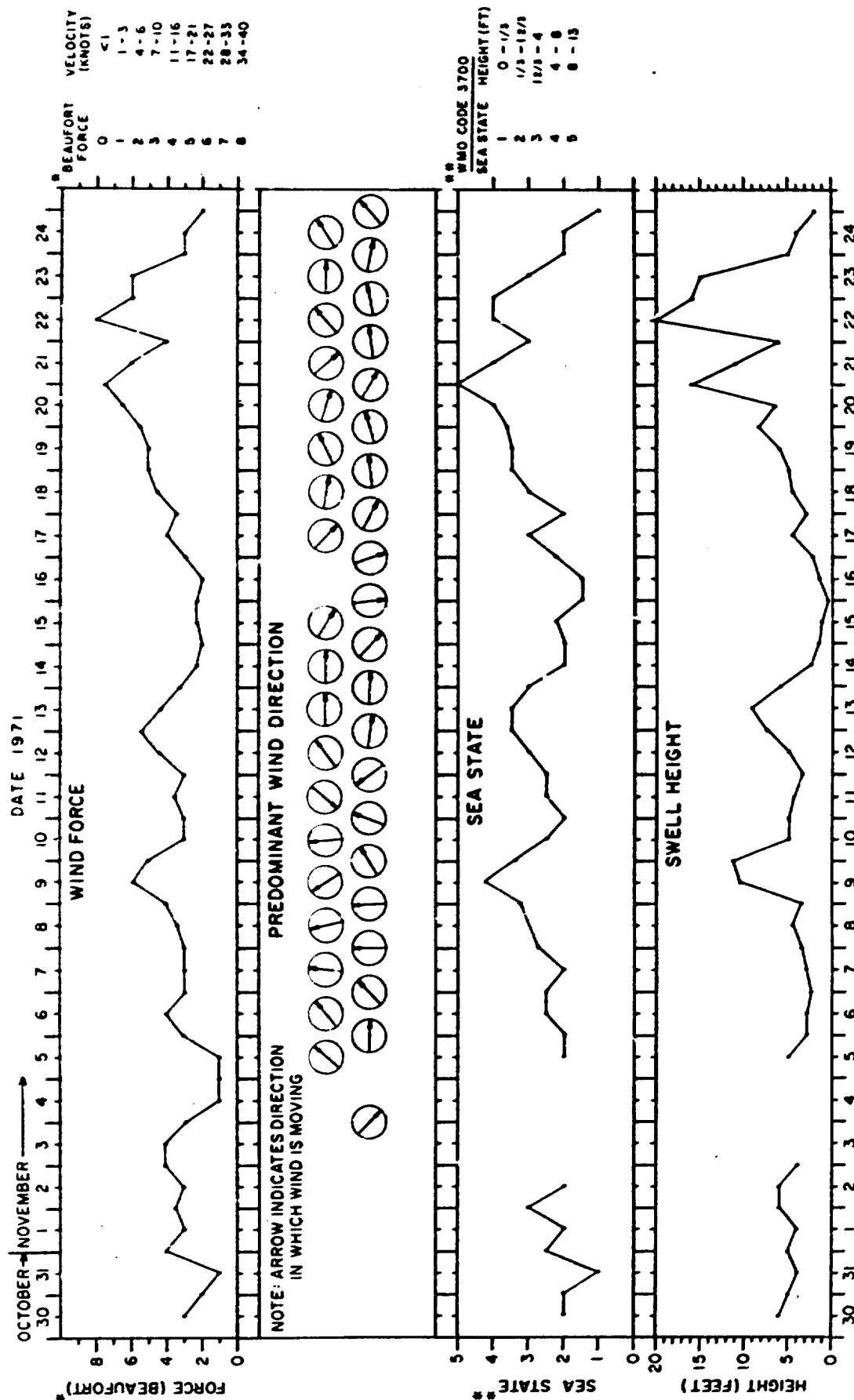


Figure 22. Wind Force, Wind Direction, Sea State, and Swell Height Summary

CONFIDENTIAL

(U) By 19 November, the exercise area was again influenced by a warm sector when a cold front passed over Sicily at about 0600Z, 20 November. The westerly winds associated with the cold front persisted through 20 and 21 November, and caused waves reaching sea state 5 (8-13 ft) associated with Beaufort 7 winds (28-33 kn). On 22 November, westerly winds still dominated the exercise area. These winds were associated with the warm sector of an occluded front centered over Denmark. Wave heights to 20 ft were observed associated with these westerly winds, and winds of up to Beaufort 8 (34-40 kn) were reported. By 0000Z on 23 November, a well-developed cold front had passed over Sicily. Well-defined westerly winds persisted until 1200Z, 23 November. A stationary front moved over the area on 24 November, and on 25 November the area again was influenced by the warm sector of an approaching cyclone.

SUMMARY

(U) During November 1971, 19 SVPs, 404 XBTs, and 153 AXBTs were collected in the Ionian Sea as part of IOMEDEX. Most of these observations were deeper than the DSC axis. Temperature traces from selected XBTs were converted into sound velocity profiles using the equation of Wilson (1960) and salinity profiles collected in the Ionian Sea during autumn 1970. Continuous bathymetric tracks were collected by six ships during IOMEDEX. In addition, NAVOCEANO implanted and recovered two current arrays at primary IOMEDEX reference points in the northern and central Ionian Sea. Wind force and direction, sea state, and swell height were observed throughout the exercise.

(C) Although large quantities of temperature and sound velocity data were collected during IOMEDEX, the majority of these data were collected synoptically with a series of scheduled acoustic measurements. Consequently, the IOMEDEX environmental data base is inadequate to resolve short-term temporal and spatial variability in near-surface thermal or vertical sound velocity structures. However, data were adequate to construct sea surface temperature contour charts for periods before and after the passage of a large storm on 19-23 November. Comparison of these charts indicates a decrease in sea surface temperature after the storm, leading to a significant decrease in critical depth. The resulting increase in depth excess leads to increasingly reliable convergence zone propagation over the course of IOMEDEX. Contour charts of mixed layer depth before and after the storm indicate that surface duct propagation is possible in most regions of the exercise area. However, short-term near-surface variability occasionally modified sound velocity gradients in the mixed layer and restricted surface duct echo ranging.

CONFIDENTIAL

(C) Oceanographic data also were adequate to define temporal changes in basic sound velocity structure at three primary IOMEDEX reference points in the northern, central, and southern Ionian Sea. The depth of the DSC axis averaged about 150 m at the reference points during the exercise. Multiple sound channels occurred at each point, but were best developed in the central Ionian Basin due to a preferential flow of high-salinity Levantine Intermediate Water (LIW). At all three points, critical depth decreased persistently during the exercise owing to autumn cooling of the near-surface layers. Depth excess at all three reference points was more than adequate for convergence zone propagation from a near-surface source throughout IOMEDEX.

(U) On the basis of IOMEDEX data, two sound velocity cross sections were constructed from 36°18'N, 17°15'E (point A) into the northern and southern Ionian Sea. On the northern section, the DSC axis varied between 90 and 200 m, and the sound velocity at the DSC axis varied between 1512.0 and 1516.1 m/sec. Maximum values of both parameters were associated with a flow of LIW extending from the Peloponnesian coast into the Ionian Sea. On the southern section, the DSC axis varied between 90 and 300 m, and sound velocity at the DSC axis varied from 1511.9 to 1517.5 m/sec. Maximum values of both parameters roughly corresponded to the major LIW flow in the Ionian Sea (Wust, 1961). Secondary sound channels above and below the DSC axis occurred frequently along both tracks. Generally, the former were caused by temperature perturbations at the base of the seasonal thermocline, and the latter were caused by mixing in the high-salinity LIW layer. Sound velocity minima below the DSC axis generally were separated from the axis by a sound velocity maximum that coincided with the LIW core. However, along the southern track, the DSC axis frequently lay below the LIW core, particularly between 34° and 35°N.

(C) Along both tracks, critical depth generally decreased northward from greater than 1400 m at the edge of the Libyan continental shelf to about 900 m in the northern Ionian Sea. Depth excess along both tracks was adequate to ensure convergence zone propagation from a near-surface source throughout the exercise. However, depth excess over the Malta Ridge (southern track) was only about 400 m, the minimum required for reliable convergence zone propagation. Significant variations in the general northward decrease in critical depth occurred between about 34°30'N and 35°00'N (southern track) and between 36°30'N and 37°30'N (northern track). In both regions, critical depth increased and then decreased rapidly to the north. These two anomalies probably were caused by meanders of the Maltese Front that separates cooler, less saline waters of the western Mediterranean Sea from warmer, more saline waters of the Ionian Sea (Johannessen, et al., 1971). Although the Maltese Front was detected during IOMEDEX (Miller, 1972), sea surface temperature data were inadequate to map the areal extent of the front.

CONFIDENTIAL

(U) At depths less than 1000 m, data collected during IOMEDEX show predominant north-northeasterly currents at 36°16'N, 17°19'E (near point A) and flows to the east-northeast and east at 38°39'N, 18°16'E (near point C). At depths below 2000 m, the current was predominantly westerly near point A and easterly near point C.

(U) Wind force, wind direction, sea state, and swell height data accurately reflect meteorological conditions in the Ionian Sea during IOMEDEX. Particularly noticeable are the effects of a large storm that passed over the central Ionian Sea between 19 and 23 November. This depression resulted in Beaufort force 8 winds (34-40 kn) and 15- to 20-foot seas. The cooler sea surface temperatures and significant mixing of the near-surface layer caused by this storm significantly decreased critical depth and comparably increased depth excess throughout the IOMEDEX area.

(C) Oceanographic conditions during IOMEDEX generally were similar to those predicted for autumn on the basis of limited pre-exercise data. Since critical depth decreased throughout the exercise, depth excess was adequate for convergence zone propagation throughout IOMEDEX. Neither the relatively shallow Malta Ridge nor the suspected presence of the Maltese Front resulted in any apparent impediment to convergence zone propagation. Depth and sound velocity of the DSC axis agreed well with historical data as shown by Brockhurst (1960) and Fenner (1968). High-salinity LIW appears to be the primary oceanographic influence on DSC structure in the Ionian Sea. This water mass also exerts a strong control on secondary sound channels below the DSC axis.

CONFIDENTIAL

UNCLASSIFIED

## REFERENCES

- Anderson, R. W., A. Fisher, Jr., and G. L. Hanssen, Analysis of airborne radiation thermometer and bathythermograph observation in the Ionian Sea during summer 1972, Tech. Note 7700-9-73, Nav. Oceanogr. Off., Washington, DC, 1973.
- Briscoe, M. G., O. M. Johannessen, and S. Vincenzi, The Maltese oceanographic front: a surface description by ship and aircraft, in SACLANT Conf. Proc., 7, 154-175, SACLANT ASW Res. Cen., La Spezia, Italy, 1972.
- Brockhurst, R. R., Notes on the acoustic structure of the eastern Mediterranean Sea (U), J. Underwater Acoust., 10(1), 7-14, 1960. CONFIDENTIAL
- Fenner, D. F., Environmental data requirements and surveillance parameters for the Mediterranean Sea (U), Requirements Document, Nav. Oceanogr. Off., Undersea Surveillance Oceanogr. Cen., Washington, DC, 1968. SECRET-NOFORN-LIMDIS
- Johannessen, O. M., F. deStrobel, and C. Gehin, Observations of an oceanic front system east of Malta in May 1971 (MAY FROST), SACLANT ASW Res. Cen., Tech. Memo. 169, La Spezia, Italy, 1971.
- Levine, E. R. and W. B. White, Thermal frontal zones in the eastern Mediterranean Sea, J. Geophys. Res., 77(6), 1081-1086, 1972.
- Matthews, D. J., Tables of the velocity of sound in pure water and sea water for use in echo-ranging and sound-ranging, Hydrog. Dep., British Admiralty, London, 1939.
- Maury Center for Ocean Science, IOMEDEX, LRAPP operation order (U), MC Plan 06, Washington, DC, 1971. CONFIDENTIAL
- Maury Center for Ocean Science, IOMEDEX synopsis (U), MC Report 07, Washington, DC, 1972a. CONFIDENTIAL
- Maury Center for Ocean Science, Mediterranean TASSRAP Exercise, final report (U), MC Report 007, Washington, DC, 1972b. SECRET-NOFORN
- Maury Center for Ocean Science, IOMEDEX summary report (U), MC Report 015, Washington, DC, 1973. CONFIDENTIAL
- Miller, A. R., P. Tcherina, H. Charnock, and D. A. McGill, Mediterranean Sea atlas of temperature-salinity-oxygen profiles and data from cruises of R/V ATLANTIS and R/V CHAIN, with distribution of nutrient chemical properties, Atlas Series, vol. III, Woods Hole Oceanogr. Inst., Woods Hole, Mass., 1970.



UNCLASSIFIED

REFERENCES (CONTINUED)

- Miller, R. R. III, Current regime of the Maltese oceanic frontal zone, Nav. Underwater Systems Center, Tech. Rep. 4381, New London, Conn., 1972.
- Moskelenko, L. V. and I. M. Ovchinnikov, Water masses of the Mediterranean Sea, Basic features of the geological structure, of the hydrologic regime, and biology of the Mediterranean Sea, 119-130, Publishing House Science, Moscow, 1965 (translated from Russian by Nav. Oceanogr. Off. Contract Translation 14, Washington, DC, 1968).
- Ovchinnikov, I. M., Circulation in the surface and intermediate waters of the Mediterranean, Oceanology, 5(1), 48-58, 1966 (translated from Russian by Amer. Geophys. Union, Washington, DC).
- Wilson, W. D., Equation for the speed of sound in sea water, J. Acoust. Soc. Am., 32(10), 1357, 1960.
- Wust, G., On the vertical circulation of the Mediterranean Sea, J. Geophys. Res., 66(10), 3261-3271, 1961.

UNCLASSIFIED

APPENDIX A  
GLOSSARY

UNCLASSIFIED

UNCLASSIFIED

AXBT - airborne expendable bathythermograph, an instrument that measures temperature as a function of depth to a maximum of 330 m

convergence zone - region where sound rays arrive at the surface in successive intervals; a mode of underwater sound propagation

critical depth - depth at which the maximum sound velocity at the surface or in the near-surface layer recurs; bottom of the DSC

depth excess - depth interval between critical depth and the sea floor (necessary for convergence zone formation)

DSC - deep sound channel; absolute sound velocity minimum

IMP - Integrated Mediterranean Plan, a series of acoustic-oceanographic exercises in the Mediterranean Sea, 1970

IOMEDEX - Ionian Mediterranean Exercise

LIW - Levantine Intermediate Water (high salinity)

mixed layer depth - depth of the bottom of the layer mixed through wave action or by thermohaline convection; the depth of the top of the thermocline (mixed layer depth does not always coincide with sonic layer depth)

surface duct - zone immediately below the sea surface where sound rays are alternately refracted towards the surface and reflected by the surface; a mode of underwater sound propagation

SVP - sound velocimeter profile; sound velocity plotted versus depth

thermocline - a vertical negative temperature gradient that is appreciably stronger than gradients above and below it (generally occurs just below the near-surface layer)

T-S - temperature-salinity

XBT - shipborne expendable bathythermograph; an instrument that measures temperature as a function of depth to either 460 m (Sippican Model T-4 probe), 760 m (T-7 probe), or 1830 m (T-5 probe)

PRECEDING PAGE BLANK-NOT FILMED

UNCLASSIFIED

APPENDIX B

HOURLY AVERAGES OF CURRENT METER MEASUREMENTS

PRECEDING PAGE BLANK NOT FILMED

UNCLASSIFIED

140400Z 16 JAN 77 195 A-34010 C/M N-444 081000FT 011220ZMOS -0007/060000  
FLAT-6AE M00K AVERAGE SPEED 04/152 DIRECTION 0100251MAG.

DIRECTION	SUM	PER.CY.
12	48	17.0
13	42	14.8
14	50	17.7
15	35	12.4
16	20	7.1
17	15	5.3
18	3	1.1
19	1	0.4
20	1	0.4
21	2	0.7
22	0	0.0
23	0	0.0
24	0	0.0
25	0	0.0
26	0	0.0
27	0	0.0
28	1	0.4
29	0	0.0
30	0	0.0
31	2	0.7
32	3	1.1
33	19	6.7
34	41	14.5

...5...10...15...20...25...30...35...40...45...50...55...60...65...70...75...80...85...90...95...100

[illegible]

**Figure B-1. Hourly Averages, Array 1, 305 m Depth**

UNCLASSIFIED

10-EDX 26 10N/17 19E ANAY+0 C/M N-470 26J00FT R/L#43HRS 0400Z/6MNV71  
FLRT-BME #809 AVERAGE SPEED CM/SEC DIRECTION DEGREES(MAG)

DIRECT. CH.	SUM	PER. CT.
9-15	40	8.3
15-30	44	9.2
30-45	72	14.9
45-60	40	8.3
60-75	30	7.4
75-90	41	8.5
90-105	35	7.2
105-120	15	3.1
120-135	9	1.9
135-150	9	1.9
150-165	6	1.2
165-180	5	1.0
180-195	1	0.2
195-210	2	0.4
210-225	1	0.2
225-240	1	0.2
240-255	1	0.2
255-270	0	0.0
270-285	0	0.0
285-300	1	0.2
300-315	21	4.3
315-330	21	4.3
330-345	20	4.0
345-360	12	2.4
360-375	12	2.4

[illegible]

**Figure B-2. Hourly Averages, Array 1, 914 m Depth**

UNCLASSIFIED

143405Z 201047198344V.1. C/M 4-474 092500T R/L=403MS 0400Z/6MSV71  
 5.01-ONE M456 AVERAGE SPEED CM/SEC DIRECTION DEGREES(MAG)

Direction	SUM	PER.CT.
1	7	1.4
2	20	3.0
3	22	3.6
4	27	5.6
5	23	4.0
6	23	4.0
7	20	4.1
8	29	6.0
9	20	6.0
10	22	6.6
11	25	5.2
12	27	5.6
13	32	6.6
14	10	2.7
15	11	2.3
16	12	2.5
17	15	3.1
18	11	2.3
19	15	3.1
20	14	2.9
21	12	2.5
22	20	4.1
23	11	2.3
24	10	2.3

[illegible]

Figure B-3. Hourly Averages, Array 1, 2804 m Depth

UNCLASSIFIED

UNCLASSIFIED

104EDEX 20 39N/18 16E ARRAY=20 C/M N=453 "50AF" R/L=40+HDS 11007/6N-V71  
 FLAT-CNE MEUR AVERAGE SPEED CM/SEC DIRECTION DEGREE(S MAG)

DIRECTION	0-15	15-30	30-45	45-60	60-75	75-90	90-105	105-120	120-135	135-150	150-165	165-180	180-195	195-210	210-225	225-240	240-255	255-270	270-285	285-300	300-315	315-330	330-345	345-360	SUM	STDEV
	2	4	2			1	1	1	1	1	1	1	1	1	1	1	1	1	1	1	1	1	1	1	16	2.9
																									29	7.1
																									17	9.1
																									55	13.5
																									45	11.1
																									70	17.2
																									45	16.0
																									45	11.1
																									27	6.6
																									7	1.7
																									5	1.2
																									1	0.2
																									0	0.0
																									2	0.5
																									1	0.2
																									0	0.0
																									0	0.0
																									1	0.2
																									0	0.0
																									0	0.0
																									0	0.0
																									1	0.2
																									2	0.5

SPEED.....0.....5.....10.....15.....20.....25.....30.....35.....40.....45.....50.....55.....60.....65.....70.....75.....80.....85.....90.....95.....100

SUM 3 23 25 56 56 70 61 67 32 9 1 1 2 0 0 0 0 0 0 0 0 0 0 0 0 0  
 PER.CT. 0.7 5.7 6.1 13.8 13.8 17.2 15.0 16.5 7.9 2.2 0.2 0.2 0.5 0.0 0.0 0.0 0.0 0.0 0.0 0.0 0.0 0.0 0.0 0.0 0.0

Figure B-4. Hourly Averages, Array 2, 152 m Depth



UNCLASSIFIED

10MEDEX 70 39N/13 16E ARRIV\*2\* C/H N-472 D\*750QFT R/L\*406MPS 1100Z/AN071  
PL0T-6NE HOUR AVERAGE SPEED CM/SEC DIRECTION DEGREES(MAG),

DIRECTION	SUM	PER.CT.
U- 15	7	1.7
15- 30	0	2.0
30- 45	11	3.7
45- 60	13	3.2
60- 75	20	4.9
75- 90	36	8.6
90-105	67	16.5
105-120	63	15.5
120-135	41	10.1
135-150	30	7.4
150-165	25	6.1
165-180	14	3.4
180-195	11	2.7
195-210	0	2.0
210-225	9	2.2
225-240	0	1.5
240-255	5	1.2
255-270	0	1.2
270-285	5	0.7
285-300	3	1.2
300-315	3	0.7
315-330	5	1.5
330-345	0	1.5
345-360	4	1.0

[illegible]

**Figure B-5. Hourly Averages, Array 2, 762 m Depth**

UNCLASSIFIED

10=0000 10 194/10 161 4949020 C/M 4-50 D=2500FT R/L=406HRS 1100Z/06NOV71  
PLOT-BNC WZ09 AVERAGE SPEED CW/SEC DIRECTION DEGREES(MAG)

Collection	Sum	Per.Ct.
30 15	15	5.2
120 30	24	5.9
120 45	33	8.1
120 60	39	7.1
60 75	27	9.1
75 90	28	6.9
90 125	29	7.1
120 120	25	6.1
120 135	26	6.9
120 150	25	6.1
120 165	18	4.4
165 180	14	2.4
180 195	11	2.7
195 210	10	2.5
210 225	2	0.5
225 240	6	1.5
240 255	5	1.3
255 270	6	1.5
270 285	9	2.2
285 300	7	1.7
300 315	15	2.7
315 330	12	2.9
330 345	14	2.4
345 360	9	2.4

PEEC...5...10...15...20...25...30...35...40...45...50...55...60...65...70...75...80...85...90...95...100

[illegible]

Figure B-6. Hourly Averages, Array 2, 2286 m Depth

UNCLASSIFIED

# DISTRIBUTION LIST

DDR&E (G. Cann) (1)

ASNR&D (1)

OCEANAV (Dr. G. Boosman) (1)

Center for Naval Analysis (1)

ARPA (K. Kressa) (1)

Inst. for Def. Analysis (1)

## ONR Codes:

102-OS (1)

102-OSC (2)

410 (1)

412 (1)

431 (1)

480 (1)

AESD (1)

CNM (NAVMAT 0341) (1)

## MASWSP (PM-4) Codes:

ASW-10 (1)

ASW-11 (1)

ASW-13 (1)

## NAVELECSYSCOM Codes:

ELEX-320 (1)

PME-124 (1)

PME-124TA (1)

PME-124-20 (1)

PME-124-30 (1)

PME-124-40 (1)

PME-124-60 (1)

NAVSEASYSYSCOM (SEA-06H1) (1)

## NRL Codes:

2627 (1)

8000 (1)

8101 (1)

8160 (1)

8174 (1)

COMNOL (1)

COMNUC (1)

NUC (Code 502) (2)

COMNAVAIRDEVCEN (1)

NAVAIRDEVCEN (Code 205) (1)

## NUSC Codes:

T (1)

TA (1)

TA111 (1)

CIC NAVFOREUR (1)

COMSIXTHFLT (1)

COMFLTAIRMED/COMASWFORSIXTHFLT (1)

COMOCEANSYSLANT (1)

COMOCEANSYSPAC (1)

COMSUBDEVGRUTWO (1)

CO FLTWEACEN ROTA (1)

CO FNWC (1)

OIC EPRF, NAVPOSTGRADSCOL (1)

DIRMPL, SIO (1)

U. Miami (Dr. S. C. Daubin) (1)

WHOI (Dr. E. E. Hayes) (1)

DDC (1)

BB&N, Inc. (C. Burroughs) (1)

B.K. Dynamics, Inc.  
(P. G. Bernard) (1)

ADL, Inc. (Dr. G. Raisbeck) (1)

Planning Systems, Inc.  
(Dr. L. P. Solomon) (1)

UNCLASSIFIED

**CONFIDENTIAL**

DISTRIBUTION LIST (CONTINUED)

Raff Assoc., Inc.  
(Dr. S. Raff) (1)

TRW Systems Group  
(Dr. R. Brown) (1)

Tetra Tech, Inc.  
(C. Dabney) (1)

TRACOR, Inc.  
(J. T. Gottwald) (1)

Underwater Systems, Inc.  
(Dr. M. S. Weinstein) (1)

Xonics, Inc.  
(S. Kulek) (1)

**CONFIDENTIAL**



**DEPARTMENT OF THE NAVY**

OFFICE OF NAVAL RESEARCH  
875 NORTH RANDOLPH STREET  
SUITE 1425  
ARLINGTON VA 22203-1995

IN REPLY REFER TO:

5510/1  
Ser 321OA/011/06  
31 Jan 06

**MEMORANDUM FOR DISTRIBUTION LIST**

Subj: DECLASSIFICATION OF LONG RANGE ACOUSTIC PROPAGATION PROJECT  
(LRAPP) DOCUMENTS

Ref: (a) SECNAVINST 5510.36

Encl: (1) List of DECLASSIFIED LRAPP Documents

1. In accordance with reference (a), a declassification review has been conducted on a number of classified LRAPP documents.
2. The LRAPP documents listed in enclosure (1) have been downgraded to UNCLASSIFIED and have been approved for public release. These documents should be remarked as follows:

Classification changed to UNCLASSIFIED by authority of the Chief of Naval Operations (N772) letter N772A/6U875630, 20 January 2006.

DISTRIBUTION STATEMENT A: Approved for Public Release; Distribution is unlimited.

3. Questions may be directed to the undersigned on (703) 696-4619, DSN 426-4619.

BRIAN LINK  
By direction

Subj: DECLASSIFICATION OF LONG RANGE ACOUSTIC PROPAGATION PROJECT  
(LRAPP) DOCUMENTS

DISTRIBUTION LIST:

NAVOCEANO (Code N121LC – Jaime Ratliff)  
NRL Washington (Code 5596.3 – Mary Templeman)  
PEO LMW Det San Diego (PMS 181)  
DTIC-OCQ (Larry Downing)  
ARL, U of Texas  
Blue Sea Corporation (Dr. Roy Gaul)  
ONR 32B (CAPT Paul Stewart)  
ONR 321OA (Dr. Ellen Livingston)  
APL, U of Washington  
APL, Johns Hopkins University  
ARL, Penn State University  
MPL of Scripps Institution of Oceanography  
WHOI  
NAVSEA  
NAVAIR  
NUWC  
SAIC

# Declassified LRAPP Documents

Report Number	Personal Author	Title	Publication Source (Originator)	Pub. Date	Current Availability	Class.
Unavailable	Beam, J. P., et al.	LONG-RANGE ACOUSTIC PROPAGATION LOSS MEASUREMENTS OF PROJECT TRANSLANT I IN THE ATLANTIC OCEAN EAST OF BERMUDA	Naval Underwater Systems Center	740612	ADC001521	U
Unavailable	Cornyn, J. J., et al.	AMBIENT-NOISE PREDICTION. VOLUME 2. MODEL EVALUATION WITH IOMEDEX DATA	Naval Research Laboratory	740701	AD0530983	U
Unavailable	Unavailable	COHERENCE OF HARMONICALLY RELATED CW SIGNALS	Naval Underwater Systems Center	740722	ADB181912	U
Unavailable	Banchero, L. A., et al.	IOMEDEX SOUND VELOCITY ANALYSIS AND ENVIRONMENTAL DATA SUMMARY	Naval Oceanographic Office	740801	ADC000419	U
3810	Unavailable	CONSTRUCTION AND CALIBRATION OF USRD TYPE F58 VIBROSEIS MONITORING HYDROPHONES SERIALS 1 THROUGH 7	Naval Research Laboratory	741002	ND	U
ARL-TM-73-11; ARL-TM-73-12	Ellis, G. E., et al.	ARL PRELIMINARY DATA ANALYSIS FROM ACODAC SYSTEM; ANALYSIS OF THE BLAKE TEST ACODAC DATA	University of Texas, Applied Research Laboratories	741015	ADA001738; ND	U
Unavailable	Mitchell, S. K., et al.	QUALITY CONTROL ANALYSIS OF SUS PROCESSING FROM ACODAC DATA	University of Texas, Applied Research Laboratories	741015	ADB000283	U
Unavailable	Unavailable	MEDEX PROCESSING SYSTEM. VOLUME II. SOFTWARE	Bunker-Ramo Corp. Electronic Systems Division	741021	ADB000363	U
Unavailable	Spofford, C. W.	FACT MODEL. VOLUME I	Maury Center for Ocean Science	741101	ADA078581	U
Unavailable	Bucca, P. J., et al.	SOUND VELOCITY STRUCTURE OF THE LABRADOR SEA, IRMINGER SEA, AND BAFFIN BAY DURING THE NORLANT-72 EXERCISE	Naval Oceanographic Office	741101	ADC000461	U
Unavailable	Anderson, V. C.	VERTICAL DIRECTIONALITY OF NOISE AND SIGNAL TRANSMISSIONS DURING OPERATION CHURCH ANCHOR	Scripps Institution of Oceanography Marine Physical Laboratory	741115	ADA011110	U
Unavailable	Baker, C. L., et al.	FACT MODEL. VOLUME II	Office of Naval Research	741201	ADA078539	U
ARL-TR-74-53	Anderson, A. L.	CHURCH ANCHOR EXPLOSIVE SOURCE (SUS) PROPAGATION MEASUREMENTS (U)	University of Texas, Applied Research Laboratories	741201	ADC002497; ND	U
MCR106	Cherkis, N. Z., et al.	THE NEAT 2 EXPERIMENT VOL 1 (U)	Maury Center for Ocean Science	741201	NS; ND	U
MCR107	Cherkis, N. Z., et al.	THE NEAT 2 EXPERIMENT VOL 2 - APPENDICES (U)	Maury Center for Ocean Science	741201	NS; ND	U
Unavailable	Mahler, J., et al.	INTERIM SHIPPING DISTRIBUTION	Tetra, Tech, BB&N, & PSI	741217	ND	U
75-9M7-VERAY-R1	Jones, C. H.	LRAPP VERTICAL ARRAY - PHASE IV	Westinghouse Electric Corp.	750113	ADA008427; ND	U
AESD-TN-75-01	Spofford, C. W.	ACOUSTIC AREA ASSESSMENT	Office of Naval Research	750201	ADA090109; ND	U